

This is the author's final, peer-reviewed manuscript as accepted for publication. The publisher-formatted version may be available through the publisher's web site or your institution's library.

A network-based meta-population approach to model Rift Valley fever epidemics

Ling Xue, H. M. Scott, Lee W. Cohnstaedt, Caterina Scoglio

How to cite this manuscript

If you make reference to this version of the manuscript, use the following information:

Xue, L., Scott, H. M., Cohnstaedt, L. W., & Scoglio, C. (2012). A network-based meta-population approach to model Rift Valley fever epidemics. Retrieved from <http://krex.ksu.edu>

Published Version Information

Citation: Xue, L., Scott, H. M., Cohnstaedt, L. W., & Scoglio, C. (2012). A network-based meta-population approach to model Rift Valley fever epidemics. *Journal of Theoretical Biology*, 306, 129-144.

Copyright: © 2012 Elsevier B.V.

Digital Object Identifier (DOI): doi:10.1016/j.jtbi.2012.04.029

Publisher's Link:

<http://www.sciencedirect.com/science/article/pii/S002251931200210X>

This item was retrieved from the K-State Research Exchange (K-REx), the institutional repository of Kansas State University. K-REx is available at <http://krex.ksu.edu>

A Network-Based Meta-Population Approach to Model Rift Valley fever Epidemics

Ling Xue^a, H. M. Scott^b, Lee W. Cohnstaedt^c, Caterina Scoglio^{a,*}

^a*Department of Electrical & Computer Engineering,
Kansas State University, U.S. 66506*

^b*Department of Diagnostic Medicine/Pathobiology,
Kansas State University, U.S. 66506*

^c*Center for Grain and Animal Health Research,
United States Department of Agriculture, U.S. 66502*

Abstract

Rift Valley fever virus (RVFV) has been expanding its geographical distribution with important implications for both human and animal health. The emergence of Rift Valley fever (RVF) in the Middle East, and its continuing presence in many areas of Africa, has negatively impacted both medical and veterinary infrastructures and human morbidity, mortality, and economic endpoints. Furthermore, worldwide attention should be directed towards the broader infection dynamics of RVFV, because suitable host, vector and environmental conditions for additional epidemics likely exist on other continents; including Asia, Europe and the Americas. We propose a new compartmentalized model of RVF and the related ordinary differential equations to assess disease spread in both time and space; with the latter driven as a function of contact networks. Humans and livestock hosts and two species of vector mosquitoes are included in the model. The model is based on weighted contact networks, where nodes of the networks represent geographical regions and the weights represent the level of contact between regional pairings for each set of species. The inclusion of human, animal, and vector movements among regions is new to RVF modeling. The movement of the infected individuals is not only treated as a possibility, but also an actuality that can be incorporated into the model. We have tested, calibrated, and evaluated the model using data from the recent 2010 RVF outbreak in South Africa as a case study; mapping the epidemic spread within and among three South African provinces. An extensive set of simulation results shows the potential of the proposed approach for accurately modeling the RVF spreading process in additional regions of the world. The benefits of the proposed model are twofold: not only can the model differentiate the maximum number of infected individuals among different provinces, but also it can reproduce the different starting times of the outbreak in multiple locations. Finally, the exact value of the reproduction number is numerically computed and upper and lower bounds for the reproduction number are analytically derived in the case of homogeneous populations.

Keywords:

networks, meta-population, deterministic model, Rift Valley fever (RVF), mitigation, *Aedes* mosquitoes, *Culex* mosquitoes

1. Introduction

Rift Valley fever (RVF) is a viral zoonosis with enormous health and economic impacts on domestic animals and humans [26], in countries where the disease is endemic and in others where sporadic epidemics and epizootics have occurred. An outbreak in South Africa in 1951 was estimated to have infected 20,000 people and killed 100,000 sheep and cattle [12, 35]. In Egypt in 1977, there were 18,000 human cases with 698 deaths resulting from the disease [12, 35]. While RVF is endemic in Africa, it also represents a threat to Europe and Western hemispheres [7, 18]. In 1997 – 1998 Kenya experienced the largest recorded outbreak with 89,000 human cases and 478 death. The first recorded outbreak outside of Africa occurred in the Arabian peninsula in 2000 – 2001 and caused 683 human cases and 95 deaths [17]. Tanzania and Somalia reported 1000 human cases and 300 deaths from an outbreak that was associated with above-normal rainfall in the region in 2006 – 2007 [17]. Rift Valley fever virus (RVFV) is generally distributed through regions of Eastern and Southern Africa where sheep and cattle are present [42]. It can cause morbidity (ranging from nondescript fever to meningo-encephalitis and hemorrhagic disease) and mortality (with case fatality rates of 0.2 – 5%) in humans [26]. The main economic losses of RVF in livestock arise due to abortion and mortality, which tends to be higher in young animals [9, 42], and bans on livestock exports during an epidemic [9, 4].

Rift Valley fever virus was first isolated from the blood of a newborn lamb in 1931 and later from the blood of adult sheep and cattle [44, 4]. Domestic ruminants and humans are among the mammalian hosts demonstrated to amplify RVFV [21] and

*Corresponding Author

Email addresses: lxue@ksu.edu (Ling Xue), hmscott@vet.k-state.edu (H. M. Scott), Lee.Cohnstaedt@ars.usda.gov (Lee W. Cohnstaedt), caterina@k-state.edu (Caterina Scoglio)

Aedes and *Culex* are believed to be the main arthropod vectors [7]. Rift Valley fever virus can be transferred vertically from females to their eggs in some species of the *Aedes* mosquitoes [18, 27]. The disease has been shown to be endemic in semi-arid zones, such as northern Senegal [45, 7, 28], and RVF epidemics often appears at 5 – 15 year cycles [28]. As noted earlier, RVFV has already spread outside Africa, to Yemen and Saudi Arabia [7, 6]. The species of vectors that are capable of transmitting RVFV have a wide global distribution [20] and there is therefore a distinct possibility for the virus to spread out of its currently expanding geographic range [9]. A pathways analysis [21] has shown that the RVF virus might be introduced into the United States in several different ways [21, 24] and that analysis identified several regions of the United States that are most susceptible to RVFV introduction. It is therefore desirable to develop effective models to better understand the potential dynamics of RVF in heretofore unaffected regions and then develop efficient mitigation strategies in case this virus appears in the Western hemisphere [18]. Such preparedness can help avoid a rapid spread of the virus throughout North America, as happened with the West Nile virus during the last decade [7, 18].

A RVF disease risk mapping model was developed by [1]. The authors observed sea surface temperature (SST) patterns, cloud cover, rainfall, and ecological indicators (primarily vegetation) via satellite data to evaluate different aspects of climate variability and their relationships to disease outbreaks in Africa and the Middle East [3, 2]. The researchers successfully predicted areas where outbreaks of RVF in humans and animals were expected using climate data for the Horn of Africa from December 2006 to May 2007. An ordinary differential equation (ODE) mathematical model was developed by [18]. The model is both an individual-based and deterministic model. The authors analyzed the stability of the model and tested the importance of the model parameters. However, neither human population parameters nor spatial (or, network) aspects are explicitly incorporated in the model. Another theoretical mathematical model on RVFV dynamic transmission was proposed [29]. This model is also an individual based model. The most important parameters to initial disease transmission and the endemic equilibrium have been carried out.

In this paper, we present a novel model incorporating *Aedes* and *Culex* mosquito vector, and livestock and human host populations. Our model is based on weighted contact networks, where nodes of the networks represent geographical regions and weights represent the level of contact between regional pairs for each vector or host species. Environmental factors such as rainfall, temperature, wind and evaporation are incorporated into the model. For each subpopulation, a set of ordinary differential equations describes the dynamics of the population in a specific geographical location, and the transitions among the different compartments, after contracting the virus. We compute the lower and upper bounds of the reproduction number for homogeneous populations, explain their biological meaning, and numerically compare the bounds with exact values.

We test, calibrate, and evaluate the model using the recent 2010 RVF outbreak in South Africa as a case study, mapping the epidemic spread in three South African provinces: Free State, Northern Cape, and Eastern Cape. An extensive set of simulation results shows the potential of the proposed approach to accurately describe the spatiotemporal evolution of RVF epidemics.

The paper is organized as follows: 1) in Section 2, we describe our compartmentalized mathematical model, present the lower bound and upper bound of the reproduction number for homogeneous populations. 2) in Section 3, we introduce the case study using outbreak data from South Africa, 2010, 3) in Section 4, we conclude our work. In the Appendix, we show how we derive the bounds for the reproduction number for homogeneous populations.

2. Compartmentalized Mathematical Model

We have constructed Compartmentalized Mathematical Models based on the principle of RVFV transmission. The parameters used in the model are shown in Table 1.

2.1. Homogeneous Populations Model

The principle of RVFV transmission between different species is shown in Figure 1. All the *Aedes* spp. and *Culex* spp. we are going to discuss only include the mosquitoes that are competent vectors of Rift Valley fever. In this paper, the *Culex* parameters are based on *Culex Tarsalis* mosquitoes and *Aedes* parameters are based on *Ae. dorsalis* mosquitoes. The main vectors, *Aedes* and *Culex* mosquitoes and the main hosts, livestock and humans are considered in the model. We use an SEI compartmental model in which individuals are either in a susceptible (S) state, an exposed (E) state, or an infected state (I) for both *Aedes* and *Culex* mosquitoes, and an SEIR compartmental model in which individuals are either in a susceptible (S) state, an exposed (E) state, an infected state (I), or a recovered (R) state for both livestock and human populations. Infectious *Aedes* mosquitoes can not only transmit RVFV to susceptible livestock and humans but also to their own eggs [18, 27]. *Culex* mosquitoes acquire the virus during blood meals on an infected animal and then amplify the transmission of RVFV through blood meals on livestock and humans [44]. Direct ruminant-to-human contact is the major (though not only) way for humans to acquire the infection [1, 11]. Accidental RVFV infections have been recorded in laboratory staff handling blood and tissue from infected animals [1]. Usually, humans are thought of as dead end hosts that do not contribute significantly to propagation of the epidemic [7]. There has been no direct human-to-human transmission of RVFV in field conditions recorded thus far [21]. The mosquitoes will not spontaneously recover once they become infectious [18]. Livestock and humans either perish from the infection or recover [18]. All four species have a specified incubation period [44]. The model is based on a daily time step. *Aedes* and *Culex*

mosquitoes are distributed among susceptible S_a , exposed E_a and infected I_a compartments. The subscript $a = 1$ denotes *Aedes* and $a = 3$ denotes *Culex*. The size of each adult mosquito population is $N_1 = S_1 + E_1 + I_1$ for adult *Aedes* mosquitoes and $N_3 = S_3 + E_3 + I_3$ for adult *Culex* mosquitoes. The livestock and human hosts contain susceptible S_b , exposed E_b , infected I_b and recovered R_b individuals. The subscript $b = 2$ and $b = 4$ denote livestock and humans respectively. The size of host populations is $N_b = S_b + E_b + I_b + R_b$. The four populations are modeled with a specified carrying capacity K_1, K_2, K_3, K_4 respectively.

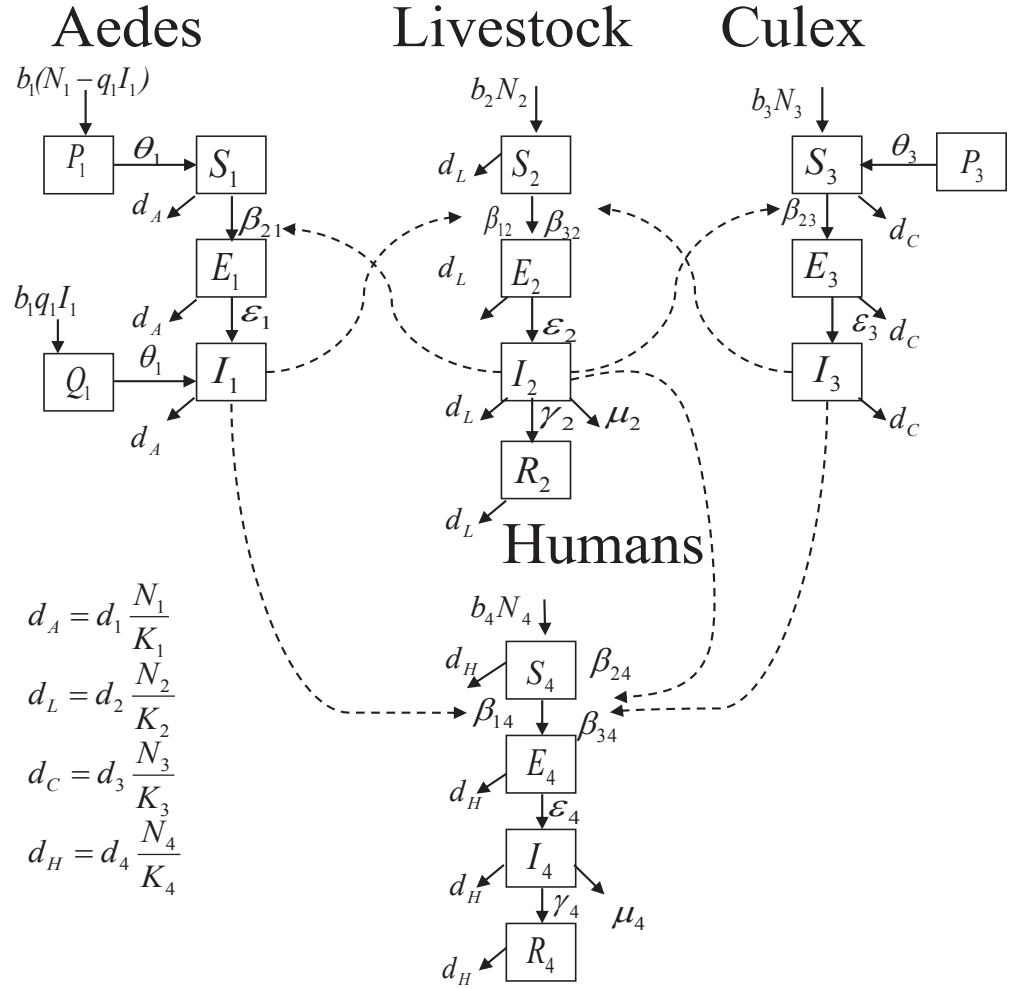


Figure 1: Flow diagram of RVFV transmission with each species, namely, *Aedes* mosquitoes, *Culex* mosquitoes, livestock, and humans homogeneously mixed (the solid lines represent transition between compartments and the dash lines represent the transmission between different species)

2.1.1. *Aedes* Mosquito Population Model

$$\begin{aligned} \frac{dP_1}{dt} &= b_1(N_1 - q_1 I_1) - \theta_1 P_1 & (1) \\ \frac{dQ_1}{dt} &= b_1 q_1 I_1 - \theta_1 Q_1 & (2) \\ \frac{dS_1}{dt} &= \theta_1 P_1 - \beta_{21} S_1 I_2 / N_2 - d_1 S_1 N_1 / K_1 & (3) \\ \frac{dE_1}{dt} &= \beta_{21} S_1 I_2 / N_2 - \epsilon_1 E_1 - d_1 E_1 N_1 / K_1 & (4) \\ \frac{dI_1}{dt} &= \theta_1 Q_1 + \epsilon_1 E_1 - d_1 I_1 N_1 / K_1 & (5) \end{aligned}$$

Parameter	Description	Value	Units	Source
β_{12}	contact rate: <i>Aedes</i> to livestock	0.002	1/day	[18]
β_{21}	contact rate: livestock to <i>Aedes</i>	0.0021	1/day	[18]
β_{23}	contact rate: livestock to <i>Culex</i>	0.000003	1/day	[18]
β_{32}	contact rate: <i>Culex</i> to livestock	0.00001	1/day	[18]
β_{14}	contact rate: <i>Aedes</i> to humans	0.000046	1/day	Assume
β_{24}	contact rate: livestock to humans	0.00017	1/day	[29]
β_{34}	contact rate: <i>Culex</i> to humans	0.0000001	1/day	Assume
γ_2	recover rate in livestock	0.14	1/day	[18]
γ_4	recover rate in humans	0.14	1/day	[39, 38, 37]
d_1	death rate of <i>Aedes</i> mosquitoes	0.025	1/day	[18]
d_2	death rate of livestock	1/3650	1/day	[18]
d_3	death rate of <i>Culex</i> mosquitoes	0.025	1/day	[18]
d_4	death rate of humans	1/18615	1/day	[39, 38, 37]
b_1	number of <i>Aedes</i> eggs laid per day	0.05	1/day	[18]
b_2	daily birthrate of livestock	0.0028	1/day	[18]
b_3	number of <i>Culex</i> eggs laid per day	weather dependent	1/day	[19]
b_4	daily birthrate of humans	1/14600	1/day	[39, 38, 37]
$1/\epsilon_1$	incubation period in <i>Aedes</i> mosquitoes	6	days	[18]
$1/\epsilon_2$	incubation period in livestock	4	days	[18]
$1/\epsilon_3$	incubation period in <i>Culex</i> mosquitoes	6	days	[18]
$1/\epsilon_4$	incubation period in humans	4	days	[44]
μ_2	mortality rate in livestock	0.0312	1/day	[18]
μ_4	mortality rate in humans	0.0001	1/day	[39, 38, 37]
q_1	transovarial transmission rate in <i>Aedes</i>	0.05	-	[18]
$1/\theta_1$	development time of <i>Aedes</i>	15	days	[18]
θ_3	development rate of <i>Culex</i>	weather dependent	1/day	[19]
K_1	carrying capacity of <i>Aedes</i> mosquitoes	1000000000	-	[32]
K_2	carrying capacity of livestock	10000000	-	Assume
K_3	carrying capacity of <i>Culex</i> mosquitoes	1000000000	-	[32]
K_4	carrying capacity of humans	10000000	-	Assume
f	fraction of those working with animals	0.82	-	[31]
τ	return rate	3	times/day	[5]
p	reduction in ω_{ij}^2 due to infection	$\frac{1}{2}$	-	Assume

Table 1: Parameters of the compartmentalized mathematical model

$$\frac{dN_1}{dt} = \theta_1(P_1 + Q_1) - d_1N_1N_1/K_1 \quad (6)$$

where:

P_1 =the number of uninfected *Aedes* mosquito eggs

Q_1 =the number of infected *Aedes* mosquito eggs

S_1 =the number of susceptible *Aedes* mosquitoes

E_1 =the number of exposed *Aedes* mosquitoes

I_1 =the number of infected *Aedes* mosquitoes

N_1 =the total number of *Aedes* mosquitoes

The above model is a modified SEI model with compartments P and Q. Compartments P and Q represent uninfected eggs and infected eggs respectively. The total number of eggs laid each day is b_1N_1 with $b_1q_1I_1$ infected eggs and $b_1N_1 - b_1q_1I_1$ uninfected eggs [18]. After development period, θ_1P_1 develop into susceptible adult mosquitoes and θ_1Q_1 develop into infected adult mosquitoes [18]. There are $d_1X_1N_1/K_1$ mosquitoes removed from compartment X due to natural death. Compartment X can be P, Q, S, E, and I here. The number of *Aedes* mosquitoes infected by livestock is denoted by $\beta_{21}S_1I_2/N_2$ which is proportional to the density of infected *Aedes* mosquitoes [18]. After incubation period, ε_1E_1 *Aedes* mosquitoes transfer to infected compartment [18].

2.1.2. Culex Mosquito Population Model

$$\frac{dP_3}{dt} = b_3N_3 - \theta_3P_3 \quad (7)$$

$$\frac{dS_3}{dt} = \theta_3P_3 - \beta_{23}S_3I_2/N_2 - d_3S_3N_3/K_3 \quad (8)$$

$$\frac{dE_3}{dt} = \beta_{23}S_3I_2/N_2 - \varepsilon_3E_3 - d_3E_3N_3/K_3 \quad (9)$$

$$\frac{dI_3}{dt} = \varepsilon_3E_3 - d_3I_3N_3/K_3 \quad (10)$$

$$\frac{dN_3}{dt} = \theta_3P_3 - d_3N_3N_3/K_3 \quad (11)$$

where:

P_3 =the number of uninfected *Culex* mosquito eggs

S_3 =the number of susceptible *Culex* mosquitoes

E_3 =the number of exposed *Culex* mosquitoes

I_3 =the number of infected *Culex* mosquitoes

N_3 =the total number of *Culex* mosquitoes

Besides compartment S, E, I, compartment P is added to represent uninfected eggs. Only uninfected eggs are included because the female *Culex* mosquitoes do not transmit RVFV vertically [18]. The total number of eggs laid each day is b_3N_3 . There are $d_3X_3N_3/K_3$ *Culex* mosquitoes removed due to natural death. Compartment X can be P, S, E, and I here. After development period, θ_3P_3 eggs develop into susceptible adult *Culex* mosquitoes and become secondary vectors [18]. The number of infected *Culex* mosquitoes from contact with livestock is denoted by $\beta_{23}S_3I_2/N_2$ which is proportional to the percentage of infected livestock [18]. After incubation period, ε_3E_3 *Culex* mosquitoes transfer from exposed compartment to infected compartment [18].

2.1.3. Livestock Population Model

$$\frac{dS_2}{dt} = b_2N_2 - d_2S_2N_2/K_2 - \beta_{12}S_2I_1/N_1 - \beta_{32}S_2I_3/N_3 \quad (12)$$

$$\frac{dE_2}{dt} = \beta_{12}S_2I_1/N_1 + \beta_{32}S_2I_3/N_3 - \varepsilon_2E_2 - d_2E_2N_2/K_2 \quad (13)$$

$$\frac{dI_2}{dt} = \varepsilon_2E_2 - \gamma_2I_2 - \mu_2I_2 - d_2I_2N_2/K_2 \quad (14)$$

$$\frac{dR_2}{dt} = \gamma_2I_2 - d_2R_2N_2/K_2 \quad (15)$$

$$\frac{dN_2}{dt} = b_2N_2 - d_2N_2N_2/K_2 - \mu_2I_2 \quad (16)$$

where:

S_2 =the number of susceptible livestock

E_2 =the number of exposed livestock

I_2 =the number of infected livestock

N_2 =the total number of livestock

There are b_2N_2 livestock born, $d_2X_2N_2/K_2$ livestock removed due to natural death [18], and μ_2I_2 livestock dying of the infection each day [18]. Compartment X can be S, E, I, and R here. Following incubation period, ε_2E_2 livestock transfer from exposed compartment to infected compartment [18]. The number of livestock infected by *Aedes* mosquitoes and *Culex* mosquitoes are denoted as $\beta_{12}S_2I_1/N_1$ and $\beta_{32}S_2I_3/N_3$ respectively [18]. Following infection period, γ_2I_2 livestock recover from RVFV infection [18].

2.1.4. Human Population Model

$$\frac{dS_4}{dt} = b_4N_4 - \beta_{14}S_4I_1/N_1 - f\beta_{24}S_4I_2/N_2 - \beta_{34}S_4I_3/N_3 - d_4S_4N_4/K_4 \quad (17)$$

$$\frac{dE_4}{dt} = \beta_{14}S_4I_1/N_1 + f\beta_{24}S_4I_2/N_2 + \beta_{34}S_4I_3/N_3 - d_4E_4N_4/K_4 - \varepsilon_4E_4 \quad (18)$$

$$\frac{dI_4}{dt} = \varepsilon_4E_4 - \gamma_4I_4 - \mu_4I_4 - d_4I_4N_4/K_4 \quad (19)$$

$$\frac{dR_4}{dt} = \gamma_4I_4 - d_4R_4N_4/K_4 \quad (20)$$

$$\frac{dN_4}{dt} = b_4N_4 - d_4N_4N_4/K_4 - \mu_4I_4 \quad (21)$$

where:

S_4 =the number of susceptible humans

E_4 =the number of exposed humans

I_4 =the number of infected humans

N_4 =the total number of humans

There are b_4N_4 humans born, $d_4X_4N_4/K_4$ humans removed from compartment X due to natural death, and μ_4I_4 humans dying of RVFV infection each day. Compartment X can be S, E, I, and R here. The number of humans that acquire the infection from *Aedes* mosquitoes, *Culex* mosquitoes, and livestock is $\beta_{14}S_4I_1/N_1$, $\beta_{34}S_4I_3/N_3$, and $f\beta_{24}S_4I_2/N_2$ respectively. We assume only those who work with animals can be infected by animals. Therefore, a coefficient f ($0 < f < 1$) which represents the fraction of humans working with animals is multiplied by $\beta_{24}S_4I_2/N_2$. After incubation period, ε_4E_4 humans transfer to infected compartment and γ_4I_4 humans transfer to recovered compartment after infection period.

2.1.5. Environmental Parameters for Culex

The equation (22) is used to model the development rate of *Culex* mosquitoes [19]. The daily egg laying rate expressed in equation (23) is a function of moisture [19]. Moisture in equation (24) is obtained by summing the difference of precipitation [30] and evaporation (mm) [25] over the proceeding 7 days [19]. In the equations (22) to (25), A , HA , HH , K , TH , E_{max} , E_{var} , E_{mean} , b_0 are parameters [19] which are described in Table 2. This model is specific for West Nile virus model in 2010 in the northern US.

$$\theta_3(Temp, t) = A * \frac{(Temp(t) + K)}{298.15} * \frac{\exp[\frac{HA}{1.987} * (\frac{1}{298.15} - \frac{1}{Temp(t)+K})]}{1 + \exp[\frac{HH}{1.987} * (\frac{1}{TH} - \frac{1}{Temp(t)+K})]} \quad (22)$$

$$b_3(Temp, precipitation, t) = b_0 + \frac{E_{max}}{1 + \exp[-\frac{Moisture(t)-E_{mean}}{E_{var}}]} \quad (23)$$

Parameter	Description	Value	Source
A	parameter of the development rate	0.25	[19]
HA	parameter of the development rate	28094	[19]
HH	parameter of the development rate	35692	[19]
TH	parameter of the development rate	298.6	[19]
b_0	minimum constant fecundity rate	3	[19]
E_{max}	maximum daily egg laying rate	3	[19]
E_{mean}	value at which moisture index=0.5 E_{max}	0	[19]
E_{var}	the variance of the daily egg laying rate	12	[19]

Table 2: Parameters of the model for *Culex*

$$Moisture(t) = \sum_{D=t-6}^t participation(D) - evaporation(D) \quad (24)$$

$$Evaporation(t) = \frac{700(Temp(t) + 0.006h)/(100 - latitude)}{80 - Temp(t)} + \frac{15(Temp(t) - T_d(t))}{80 - Temp(t)} mm/day \quad (25)$$

Where:

$Temp(t)$ =air temperature in units of $^{\circ}C$ [25]

$latitude$ =the latitude (degrees) [25]

$T_d(t)$ =the mean dew-point in units of $^{\circ}C$ [25]

h =the elevation (meters) [25]

K = Kelvin parameter [25]

2.1.6. The Reproduction Number for Homogeneous Populations

The reproduction number R_0 is defined as: “ The average number of secondary cases arising from an average primary case in an entirely susceptible population” [14]. The reproduction number is used to predict whether the epidemic will spread or die out. There are several methods used to compute R_0 . One of these methods computes the reproduction number as the spectral radius [14?] of the next generation matrix [14?].

The next generation matrix is defined as FV^{-1} , and the matrices F and V are determined as:

$$F = \left[\frac{\partial \mathcal{F}_i(x_0)}{\partial x_j} \right], \quad V = \left[\frac{\partial \mathcal{V}_i(x_0)}{\partial x_j} \right]$$

where x_j is the number or proportion of infected individuals in compartment j , $j = 1, 2, 3, \dots, m$, m being the total number of infected compartments, x_0 is the disease free equilibrium vector, \mathcal{F}_i is the rate of appearance of new infections in compartment i , and $\mathcal{V}_i = \mathcal{V}_i^- - \mathcal{V}_i^+$ with \mathcal{V}_i^- denoting the transfer of individuals out of compartment i and \mathcal{V}_i^+ denoting the rate of transfer of individuals into compartment i [16]. The (i, j) entry of F represents the rate at which infected individuals in compartment j produce infected individuals in compartment i [16]. The (j, k) entry of V^{-1} represents the average time that an individual spends in compartment j , where $i, j, k = 1, 2, 3, \dots, m$ [16]. Finally, the (i, k) entry of FV^{-1} represents the expected number of infected individuals in compartment i produced by the infected individuals in compartment k [16].

For our homogeneous population model, we found that

$$R_0^H \leq R_0 \leq R_0^H + q_1 \quad (26)$$

where

$$R_0^H = \sqrt{\frac{\varepsilon_2}{(b_2 + \varepsilon_2)(b_2 + \gamma_2 + \mu_2)} \left[\frac{\varepsilon_1 \beta_{12} \beta_{21}}{b_1(b_1 + \varepsilon_1)} + \frac{\varepsilon_3 \beta_{32} \beta_{23}}{b_3(b_3 + \varepsilon_3)} \right]} \quad (27)$$

See the Appendix for the derivation details, the biological interpretation, and the comparison among exact values and bounds for the reproduction number.

2.2. Meta-Population Model

A meta-population model is a model with several subpopulations. It assumes homogeneity within each subpopulation and heterogeneity among different subpopulations. The *Aedes* and *Culex* mosquitoes in location i ($i = 1, 2, 3, \dots, n$), are distributed among susceptible S_{ai} , exposed E_{ai} and infected I_{ai} compartments. The subscript $a = 1$ denotes *Aedes* and $a = 3$ denotes *Culex*. The size of each adult mosquito population in location i is $N_{1i} = S_{1i} + E_{1i} + I_{1i}$ for adult *Aedes* mosquitoes and $N_{3i} = S_{3i} + E_{3i} + I_{3i}$ for adult *Culex* mosquitoes. The livestock and human hosts contain susceptible S_{bi} , exposed E_{bi} , infected I_{bi} and recovered R_{bi} individuals. The subscript $b = 2$ and $b = 4$ denote the livestock and humans, respectively. The size of host populations in location i is $N_{2i} = S_{2i} + E_{2i} + I_{2i} + R_{2i}$ for livestock hosts and $N_{4i} = S_{4i} + E_{4i} + I_{4i} + R_{4i}$ for human hosts. The four populations are modeled with a specified carrying capacity K_1, K_2, K_3, K_4 respectively.

2.2.1. Movement between Nodes

We used weighted networks for each compartment of the four species as is shown in Figure 2. The superscripts of ω on the left hand side of equations (28), (29), and (31) represent the movement of different species. The number '1' in the superscript means the movement of *Aedes* or *Culex* population, '2' means the livestock movement, and '3' means the human movement in the superscript. The subscript ij of ω_{ij} means that the direction of the movement is from location i to location j . The difference in the thickness of the lines represent the difference in weight. Thicker lines represent the larger weight. The weight for each population is between 0 and 1. RVFV has been documented to be spread by wind [35]. Wind dispersal of mosquitoes has changed geographic distribution and accelerated the spread of RVFV to new geographic areas [21]. Some locations can become secondary epidemic sites after the virus has been introduced (especially in irrigated areas, e.g. Gazeera in Sudan or rice valleys in the center of Madagascar) [28]. Livestock trade and transport also can affect the geographic distribution of RVF [7]. One critical objective in developing effective models is to determine the major factors involved in the disease spreading process. Therefore, we parameterize the weight due to mosquito movement with wind [21, 8], livestock movement due to transportation to feedlots or trade centers [40], and human mobility due to commuting [5] as shown in equations (28), (29), and (31), respectively. The movement rate of infected livestock is reduced due to infection [44]. We use the wind data [41] in Bloemfontein, which is the capital of Free State, as the wind of Free State Province, that of Kimberley, which is the capital of Northern Cape, as the wind of Northern Cape Province and that of Grahams town, which is the center of Eastern Cape Province, as the wind of Eastern Cape Province. The distance vector is calculated with longitude and latitude in the center of each location. The number of animals sold [37] and the number of livestock in the feedlots [34] are factors of weight for livestock movement. Distance, human population, commuting rate, and return rate [39] affect the weight for human movement. Weight for mosquito movement is decided by distance and the projection of wind in the direction of distance vector [8].

$$\omega_{ij}^1 = c_1 \frac{\vec{W}_i \cdot \vec{D}_{ij}}{|\vec{D}_{ij}|} \frac{1}{|\vec{D}_{ij}|} \quad (28)$$

$$\omega_{ij}^2 = c_2 \frac{FM_j}{FM_i} \frac{1}{|\vec{D}_{ij}|} \quad (29)$$

$$\sigma_{ij} = c_3 \frac{N_{4i}^\alpha N_{4j}^\gamma}{e^{\beta|\vec{D}_{ij}|}} \quad (30)$$

$$\omega_{ij}^3 = \frac{\sigma_{ij}}{N_{4i}} \quad (31)$$

$$\omega_i = \sum_{j=1, j \neq i}^n \omega_{ij}^3 \quad (32)$$

Here:

\vec{W}_i = the wind vector in location i [8]

\vec{D}_{ij} = the distance vector from location i to location j

$\omega_{ij}^1(t)$ = the weight for mosquitoes moving from location i to location j

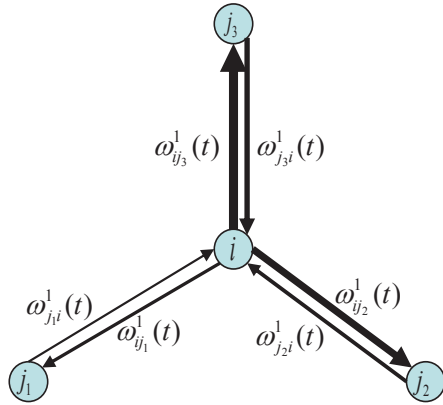
$\omega_{ij}^2(t)$ = the weight for livestock moving from location i to location j

$\sigma_{ij}(t)$ = the number of commuters between location i and location j

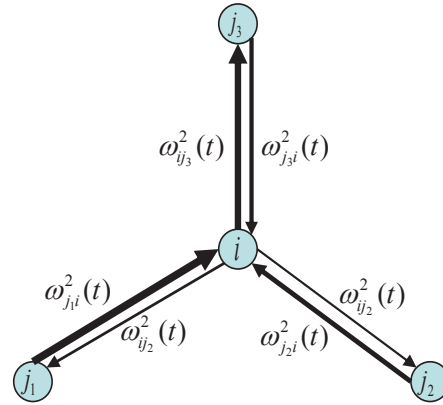
FM_i = the number of animals in markets and feedlots in location i

2.2.2. *Aedes* Movement between Nodes

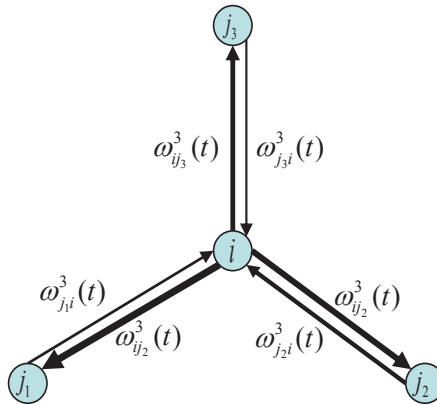
$$\frac{dP_{1i}}{dt} = b_1 (N_{1i} - q_1 I_{1i}) - \theta_1 P_{1i} \quad (33)$$



(a) Mosquito movement network (Mosquitoes can move from node i to node j_1 , j_2 , and j_3 and vice versa due to wind. We assume mosquitoes do not return to the node they are from.)



(b) Livestock movement network (Livestock can move from node i to node j_1 , j_2 , and j_3 and vice versa due to trade. We assume livestock do not return to the node they are from.)



(c) Human movement network (Humans can commute from node i to node j_1 , j_2 , and j_3 and vice versa. We assume humans return to the node they are from.)

Figure 2: Network graphs with node i which has three neighbors as an example

$$\frac{dQ_{1i}}{dt} = b_1 q_1 I_{1i} - \theta_1 Q_{1i} \quad (34)$$

$$\frac{dS_{1i}}{dt} = \theta_1 P_{1i} - \beta_{21} S_{1i} I_{2i} / N_{2i} - d_1 S_{1i} N_{1i} / K_1 + \sum_{j=1, j \neq i}^n \omega_{ji}^1 S_{1j} - \sum_{j=1, j \neq i}^n \omega_{ij}^1 S_{1i} \quad (35)$$

$$\frac{dE_{1i}}{dt} = \beta_{21} S_{1i} I_{2i} / N_{2i} - \varepsilon_1 E_{1i} - d_1 E_{1i} N_{1i} / K_1 + \sum_{j=1, j \neq i}^n \omega_{ji}^1 E_{1j} - \sum_{j=1, j \neq i}^n \omega_{ij}^1 E_{1i} \quad (36)$$

$$\frac{dI_{1i}}{dt} = \theta_1 Q_{1i} + \varepsilon_1 E_{1i} - d_1 I_{1i} N_{1i} / K_1 + \sum_{j=1, j \neq i}^n \omega_{ji}^1 I_{1j} - \sum_{j=1, j \neq i}^n \omega_{ij}^1 I_{1i} \quad (37)$$

$$\begin{aligned} \frac{dN_{1i}}{dt} = & \theta_1 (P_{1i} + Q_{1i}) - d_1 N_{1i} N_{1i} / K_1 + \sum_{j=1, j \neq i}^n \omega_{ji}^1 S_{1j} - \sum_{j=1, j \neq i}^n \omega_{ij}^1 S_{1i} + \sum_{j=1, j \neq i}^n \omega_{ji}^1 E_{1j} \\ & - \sum_{j=1, j \neq i}^n \omega_{ij}^1 E_{1i} + \sum_{j=1, j \neq i}^n \omega_{ji}^1 I_{1j} - \sum_{j=1, j \neq i}^n \omega_{ij}^1 I_{1i} \end{aligned} \quad (38)$$

The change in the number of *Aedes* mosquitoes due to mobility in compartment X is given as $\sum_{j=1, j \neq i}^n \omega_{ji}^1 X_{1j} - \sum_{j=1, j \neq i}^n \omega_{ij}^1 X_{1i}$ [22].

2.2.3. *Culex* Movement between Nodes

$$\frac{dP_{3i}}{dt} = b_3 N_{3i} - \theta_3 P_{3i} \quad (39)$$

$$\frac{dS_{3i}}{dt} = \theta_3 P_{3i} - \beta_{23} S_{3i} I_{2i} / N_{2i} - d_3 S_{3i} N_{3i} / K_3 + \sum_{j=1, j \neq i}^n \omega_{ji}^1 S_{3j} - \sum_{j=1, j \neq i}^n \omega_{ij}^1 S_{3i} \quad (40)$$

$$\frac{dE_{3i}}{dt} = \beta_{23} S_{3i} I_{2i} / N_{2i} - \varepsilon_3 E_{3i} - d_3 E_{3i} N_{3i} / K_3 + \sum_{j=1, j \neq i}^n \omega_{ji}^1 E_{3j} - \sum_{j=1, j \neq i}^n \omega_{ij}^1 E_{3i} \quad (41)$$

$$\frac{dI_{3i}}{dt} = \varepsilon_3 E_{3i} - d_3 I_{3i} N_{3i} / K_3 + \sum_{j=1, j \neq i}^n \omega_{ji}^1 I_{3j} - \sum_{j=1, j \neq i}^n \omega_{ij}^1 I_{3i} \quad (42)$$

$$\begin{aligned} \frac{dN_{3i}}{dt} = & \theta_3 P_{3i} - d_3 N_{3i} N_{3i} / K_3 + \sum_{j=1, j \neq i}^n \omega_{ji}^1 S_{3j} - \sum_{j=1, j \neq i}^n \omega_{ij}^1 S_{3i} + \sum_{j=1, j \neq i}^n \omega_{ji}^1 E_{3j} \\ & - \sum_{j=1, j \neq i}^n \omega_{ij}^1 E_{3i} + \sum_{j=1, j \neq i}^n \omega_{ji}^1 I_{3j} - \sum_{j=1, j \neq i}^n \omega_{ij}^1 I_{3i} \end{aligned} \quad (43)$$

The change in the number of *Culex* mosquitoes in compartment X due to movement is given as $\sum_{j=1, j \neq i}^n \omega_{ji}^1 X_{3j} - \sum_{j=1, j \neq i}^n \omega_{ij}^1 X_{3i}$ [22].

2.2.4. *Livestock* Movement between Nodes

$$\frac{dS_{2i}}{dt} = b_2 N_{2i} - \beta_{12} S_{2i} I_{1i} / N_{1i} - \beta_{32} S_{2i} I_{3i} / N_{3i} - d_2 S_{2i} N_{2i} / K_2 + \sum_{j=1, j \neq i}^n \omega_{ji}^2 S_{2j} - \sum_{j=1, j \neq i}^n \omega_{ij}^2 S_{2i} \quad (44)$$

$$\frac{dE_{2i}}{dt} = \beta_{12} S_{2i} I_{1i} / N_{1i} + \beta_{32} S_{2i} I_{3i} / N_{3i} - \varepsilon_2 E_{2i} - d_2 E_{2i} N_{2i} / K_2 + \sum_{j=1, j \neq i}^n \omega_{ji}^2 E_{2j} - \sum_{j=1, j \neq i}^n \omega_{ij}^2 E_{2i} \quad (45)$$

$$\frac{dI_{2i}}{dt} = p \sum_{j=1, j \neq i}^n \omega_{ji}^2 I_{2j} - p \sum_{j=1, j \neq i}^n \omega_{ij}^2 I_{2i} - d_2 I_{2i} N_{2i} / K_2 + \varepsilon_2 E_{2i} - \gamma_2 I_{2i} - \mu_2 I_{2i} \quad (46)$$

$$\frac{dR_{2i}}{dt} = \sum_{j=1, j \neq i}^n \omega_{ji}^2 R_{2j} - \sum_{j=1, j \neq i}^n \omega_{ij}^2 R_{2i} + \gamma_2 I_{2i} - d_2 R_{2i} N_{2i} / K_2 \quad (47)$$

$$\begin{aligned} \frac{dN_{2i}}{dt} = & b_2N_{2i} - d_2N_{2i}N_{2i}/K_2 - \mu_2I_{2i} + \sum_{j=1, j \neq i}^n \omega_{ji}^2 S_{2j} - \sum_{j=1, j \neq i}^n \omega_{ij}^2 S_{2i} + \sum_{j=1, j \neq i}^n \omega_{ji}^2 E_{2j} \\ & - \sum_{j=1, j \neq i}^n \omega_{ij}^2 E_{2i} + p \sum_{j=1, j \neq i}^n \omega_{ji}^2 I_{2j} - p \sum_{j=1, j \neq i}^n \omega_{ij}^2 I_{2i} + \sum_{j=1, j \neq i}^n \omega_{ji}^2 R_{2j} - \sum_{j=1, j \neq i}^n \omega_{ij}^2 R_{2i} \end{aligned} \quad (48)$$

The change in the number of animals due to movement in susceptible, exposed, and recovered compartment is $\sum_{j=1, j \neq i}^n \omega_{ji}^2 X_{2j} - \sum_{j=1, j \neq i}^n \omega_{ij}^2 X_{2i}$ [22] for livestock. Concerning the animals in the infected compartment, we assume that the movement rate of the infected livestock is p ($0 < p < 1$) of livestock in other compartments. This value of the movement rate has been selected in the absence of further information.

2.2.5. Human Movement between Nodes

$$\begin{aligned} \frac{dS_{4i}}{dt} = & b_4N_{4i} - d_4S_{4i}N_{4i}/K_4 - \frac{\beta_{14}S_{4i}I_{1i}/N_{1i}}{1 + \sigma_i/\tau} - \frac{\beta_{24}fS_{4i}I_{2i}/N_{2i}}{1 + \sigma_i/\tau} - \frac{\beta_{34}S_{4i}I_{3i}/N_{3i}}{1 + \sigma_i/\tau} \\ & - \sum_{j=1, j \neq i}^n \frac{\beta_{14}S_{4i}I_{1j}/N_{1j}\sigma_{ij}/\tau}{1 + \sigma_i/\tau} - \sum_{j=1, j \neq i}^n \frac{\beta_{24}fS_{4i}I_{2j}/N_{2j}\sigma_{ij}/\tau}{1 + \sigma_i/\tau} - \sum_{j=1, j \neq i}^n \frac{\beta_{34}S_{4i}I_{3j}/N_{3j}\sigma_{ij}/\tau}{1 + \sigma_i/\tau} \end{aligned} \quad (49)$$

$$\begin{aligned} \frac{dE_{4i}}{dt} = & \frac{\beta_{14}S_{4i}I_{1i}/N_{1i}}{1 + \sigma_i/\tau} + \frac{\beta_{24}fS_{4i}I_{2i}/N_{2i}}{1 + \sigma_i/\tau} + \frac{\beta_{34}S_{4i}I_{3i}/N_{3i}}{1 + \sigma_i/\tau} + \sum_{j=1, j \neq i}^n \frac{\beta_{14}S_{4i}I_{1j}/N_{1j}\sigma_{ij}/\tau}{1 + \sigma_i/\tau} \\ & + \sum_{j=1, j \neq i}^n \frac{\beta_{24}fS_{4i}I_{2j}/N_{2j}\sigma_{ij}/\tau}{1 + \sigma_{ij}/\tau} + \sum_{j=1, j \neq i}^n \frac{\beta_{34}S_{4i}I_{3j}/N_{3j}\sigma_{ij}/\tau}{1 + \sigma_i/\tau} - d_4E_{4i}N_{4i}/K_4 - \varepsilon_4E_{4i} \end{aligned} \quad (50)$$

$$\frac{dI_{4i}}{dt} = \varepsilon_4E_{4i} - \gamma_4I_{4i} - \mu_4I_{4i} - d_4I_{4i}N_{4i}/K_4 \quad (51)$$

$$\frac{dR_{4i}}{dt} = \gamma_4I_{4i} - d_4R_{4i}N_{4i}/K_4 \quad (52)$$

$$\frac{dN_{4i}}{dt} = b_4N_{4i} - d_4N_{4i}N_{4i}/K_4 - \mu_4I_{4i} \quad (53)$$

The humans from location i can stay in location i or move to location j at time t [5]. The number of humans infected by *Aedes* mosquitoes, *Culex* mosquitoes and livestock is $\beta_{14}(S_{4ii} \frac{I_{1i}}{N_{1i}} + \sum_{j=1, j \neq i}^n S_{4ij} \frac{I_{1j}}{N_{1j}})$ [5], $\beta_{34}(S_{4ii} \frac{I_{3i}}{N_{3i}} + \sum_{j=1, j \neq i}^n \beta_{34}S_{4ij} \frac{I_{3j}}{N_{3j}})$ [5], and $f\beta_{24}(S_{4ii} \frac{I_{2i}}{N_{2i}} + \sum_{j=1, j \neq i}^n S_{4ij} \frac{I_{2j}}{N_{2j}})$ [5] respectively.

where:

S_{4ii} = the number of humans that are from location i and stay in location i at time t [5].

S_{4ij} = the number of humans that are from location i and stay in location j at time t [5].

ω_{ij}^3 = the commuting rate between subpopulation i and each of its neighbor j [5]

ω_i = daily total rate of commuting for population i [5]

The change in the number of susceptible humans that are from location i and stay in location i is given [5] by the following expression.

$$\frac{\partial S_{4ii}}{\partial t} = \sum_{j=1, j \neq i}^n \tau S_{4ij} - \sum_{j=1, j \neq i}^n \omega_{ij}^3 S_{4ii}$$

The change in the number of susceptible humans that are from location i and stay in location j is given [5] by the following expression.

$$\frac{\partial S_{4ij}}{\partial t} = \omega_{ij}^3 S_{4ii} - \tau S_{4ij}$$

We can get the solution of S_{4ii} and S_{4ij} through the above two equations at the equilibrium.

$$S_{4ii} = \frac{S_{4i}}{1 + \omega_i/\tau} \quad (54)$$

$$S_{4ij} = \frac{S_{4i}}{1 + \omega_i/\tau} \omega_{ij}^3/\tau \quad (55)$$

3. Case Study: South Africa 2010

We have used data from the South African RVF outbreak in 2010 as a case study.

3.1. Incidence Data Analysis

Outbreak data for animals are obtained from [15, 43], while outbreak data for human subpopulations are collected from [13, 31]. As far as animal data is concerned, we chose to analyze RVF incidence in the sheep population. Because the granularity of human incidence data is provided at Province level, each node in the network represents a province. We selected three provinces: Free State (location 1), Northern Cape (location 2) and Eastern Cape (location 3), because they had the highest levels of RVF incidence for humans. The curves of the incidence data are shown in Figure 3 using green histograms, while the red curves represent simulations obtained with our model. From the data in Figure 3, it is possible to observe that the epidemic started first in the Free State Province and later in Northern Cape Province. The sustained heavy rainfall likely triggered the outbreak, causing infected eggs to hatch in the Free State Province. Additionally, the number of animal and human cases in Eastern Cape Province is smaller than the other two provinces.

3.2. Sensitivity Analysis

The three parameters c_1 , c_2 and c_3 are estimated using the least square approach, which is based on minimization of errors between the incidence data of humans and the percentage of humans calculated by the mathematical model. At first, we establish an objective function. At each sample time, we calculate the difference between the number of humans calculated by differential equations and that reported [36] during outbreaks in three provinces of South Africa from January, 2010. We calculate the square of each difference. Then, we add all the squares for each location in each day together to obtain the objective function as is shown below. Minimization of the objective function is initiated by providing initial values c_{10} , c_{20} and c_{30} for each parameter. The differential equations are solved with each set of the parameters and the square errors between the number of infected humans obtained from the objective function and those from incidence data are calculated. The parameters c_1 , c_2 and c_3 we used in the model are $c_1 = 0.009$, $c_2 = 0.05$ and $c_3 = 0.005$.

$$F = \sum_{t=t_0}^{t_f} \sum_{i=1}^n [(I_{4i}(t) - PR_{4i}(t))^2] \quad (56)$$

In the equations above,

n = the number of nodes

t_0 =starting time

t_f =end time

$I_{4i}(t)$ =human prevalence calculated by the model

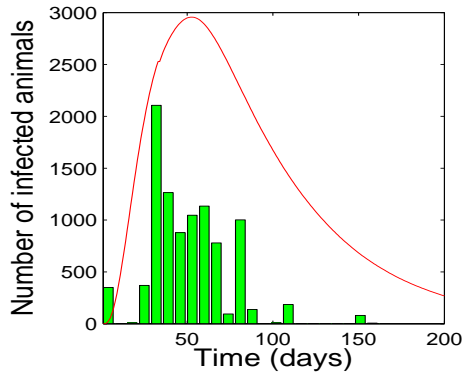
$PR_{4i}(t)$ =human prevalence reported

To conduct a sensitivity analysis of the parameters c_1 , c_2 , and c_3 in equations (28), (29), and (31), we have changed each parameter within $\pm 10\%$ of the values $c_1 = 0.009$, $c_2 = 0.05$ and $c_3 = 0.005$, keeping the other parameters constant. This analysis allows an evaluation of the impact of uncertainties in the parameter estimations. The percentage of infected humans obtained from simulation with $c_1 = 0.009$, $c_2 = 0.05$ and $c_3 = 0.005$ is represented as $I_{O_i}(t)$. The percentage of infected human obtained from simulation with the parameters within $\pm 10\%$ bound is represented as $I_{4i}(t)$. The relative errors between the fractions of infected humans are calculated for each set of parameters, in each location, at time t as $|\frac{I_{4i}(t) - I_{O_i}(t)}{I_{4i}(t)}|$. The relative errors and the lower bound and upper bound of the parameters are shown in Figure 4.

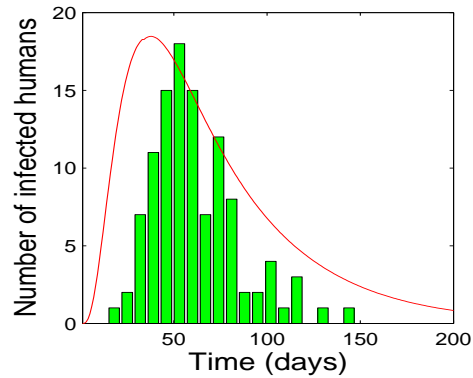
All the values of relative errors shown in Figure 4 are smaller than 10%, proving the model robustness with respect to limited uncertainties in the parameter estimation. The rest of the parameters such as contact rate β_{12} , β_{21} , β_{23} , β_{32} , death rate d_1 , d_3 and recovery rate γ_2 are the most significant parameters in [18]. Similarly, β_{14} , β_{24} , β_{34} and γ_4 are also the most significant parameters in this model.

3.3. Analysis of Simulation Results

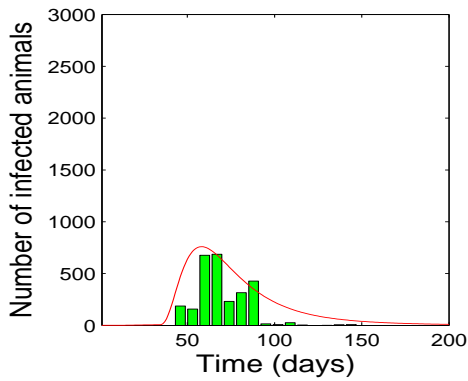
To explore the behavior of RVFV, we conducted numerical simulations of an open system considering movement of the four species among different locations. To test the validity of the model, we changed some parameters in the weights to see the impact of each variation. If the number of infected eggs $Q_{11} = 10$, $Q_{12} = 0$, and $Q_{13} = 0$, at the beginning infected eggs only exist in location 1, Free State. However, our model considers movement of mosquitoes to other locations with wind. As a consequence, infected animals and humans appear in all three locations as is shown in Figure 5. Therefore, the infection spreads due to movement of the four populations.



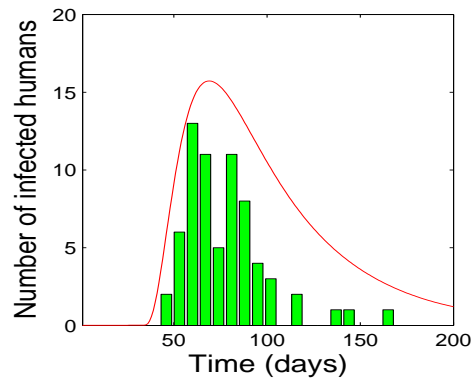
(a) Simulation result and incidence data for sheep in Free State Province



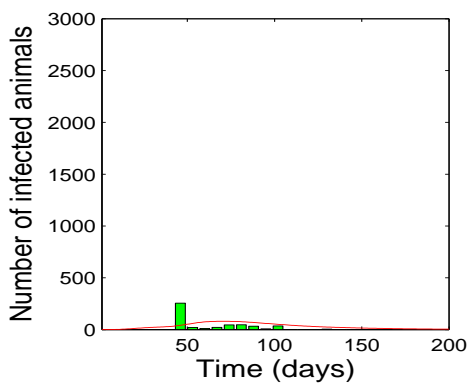
(b) Simulation result and incidence data for humans in Free State Province



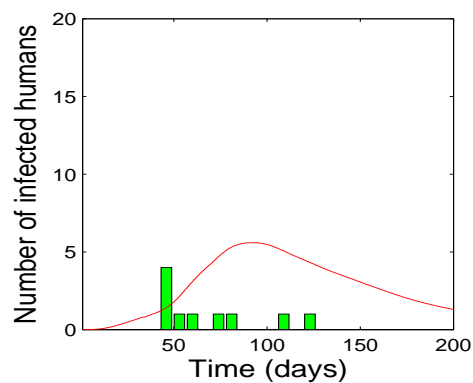
(c) Simulation result and incidence data for sheep in Northern Cape Province



(d) Simulation result and incidence data for humans in Northern Cape Province



(e) Simulation result and incidence data for sheep in Eastern Cape Province



(f) Simulation result and incidence data for humans in Eastern Cape Province

Figure 3: Simulation results and incidence data from January, 2010 in South Africa (bars are data and lines are simulation results)

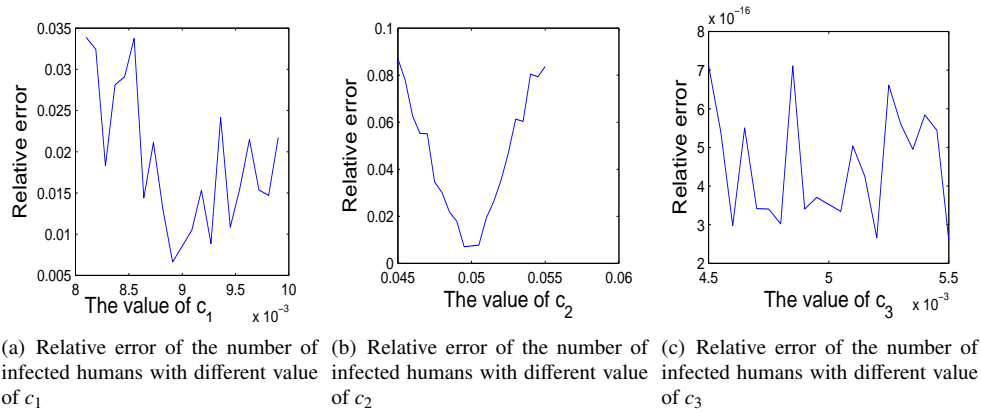


Figure 4: The relative error of the number of infected humans with changing one of the parameters c_1 , c_2 , and c_3

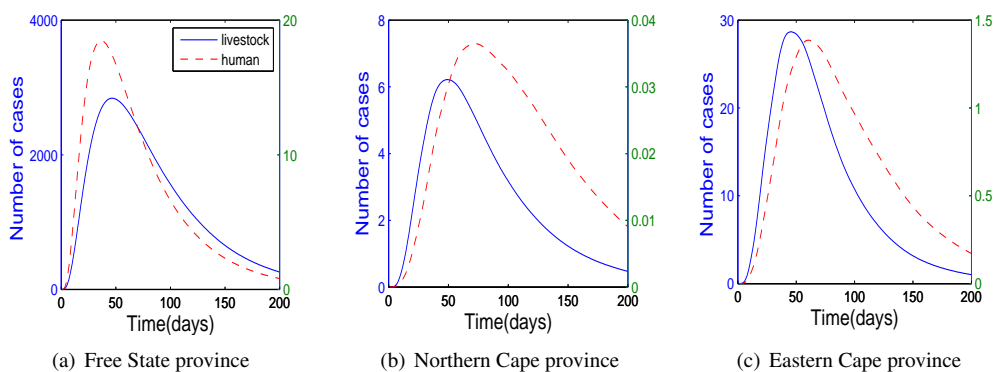


Figure 5: Simulation results with nonzero movement weights (the solid line represents livestock with y-axis on the left and the dash line represents humans with y-axis on the right)

If we also assume that at the beginning infected eggs only exist in location 1, $Q_{11} = 10$, $Q_{12} = 0$ and $Q_{13} = 0$, and movements of the four species from one location to another are not allowed, $c_1 = 0$, $c_2 = 0$, and $c_3 = 0$, then infected animals and humans will not appear in location 2 and location 3 as is shown in Figure 6. We can test the mitigation strategy of movement ban with this model. We performed the simulations to reproduce the RVFV outbreak in the three South African Provinces. The simulation results and the incidence data are shown in Figure 3. The model can differentiate the maximum number of infected individuals among the three different provinces, it also reproduces the different starting time of the outbreak in the three locations. With a homogeneous population model, such as the one in [18], the spatial differentiation is not possible.

The animal incidence curves provided by the model were always an overestimation of the data, since underreporting is very common during outbreaks. Finally, our approach in which the fractions of each subpopulation in each compartment are expressed as continuous variables, requires a large number of cases to be accurate. For this reason, the incidence data for location 3, Eastern Cape, are better approximated by a stochastic model. The model has shown the ability of fitting the data. The starting time and trend of outbreak dynamics have been reproduced by the model.

4. Conclusions

A meta-population, network-based, deterministic RVFV model is presented here. The animal, human and mosquito movement and their spatial distribution are considered by the model. The model successfully describes a real outbreak dynamics of RVFV, taking into account space and movement. When considering n locations or nodes ($n \geq 1$), there are $21 * n$ differential equations and $21 * n$ variables in our model, while there are only 14 equations with 14 variables in the model presented in [29] and 16 equations with 16 variables presented in [18]. Greater accuracy of our model is obtained at the cost of an increased complexity. The novelty of our model is that it considers a weighted contact network to represent the movement of four species. Subpopulations at the node level are also incorporated in our model. Additionally, parameters representing mosquito propagation and development are not constant but are the functions of climate factors. The model has been evaluated using data from the recent outbreak in South Africa. We reproduced not only the starting time but also the trend of RVFV transmission with time in different locations.

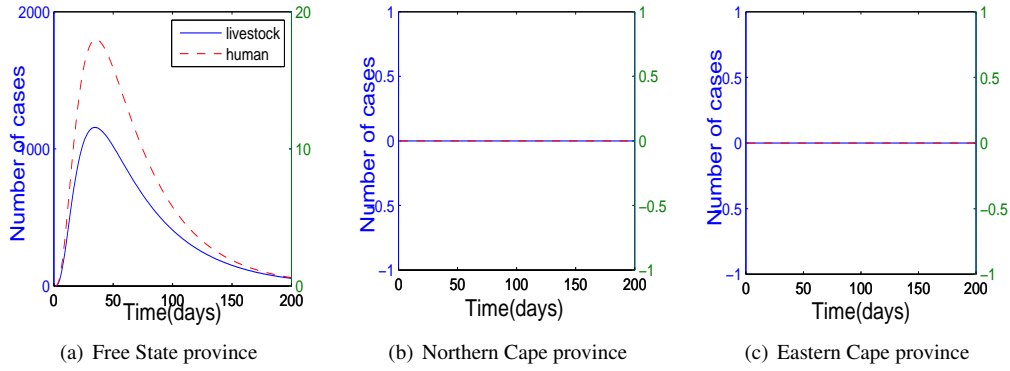


Figure 6: Simulation results with $c_1 = c_2 = c_3 = 0$ (the solid line represents livestock with y-axis on the left and the dash line represents humans with y-axis on the right)

The model has shown to be very promising notwithstanding the limitation of the data. Due to the flexibility and accuracy of the proposed model, we can test and design multiple and different mitigation strategies in different locations at different times. The lower bound and upper bound of the reproduction number for homogeneous populations are shown to be very close to the exact value, and they provide insights on the biology of the spreading process. Future work in follow-up mathematical models includes the development of a stochastic model, the study of the impact of climate changes on the epidemiology and control of RVF, and the improvement of the mosquito movement model considering diffusion equations. Moreover, the carrying capacities of mosquitoes will be considered dependent on climate factors in the future.

Acknowledgments

This work has been supported by the DHS Center of Excellence for Emerging and Zoonotic Animal Diseases (CEEZAD), and by the National Agricultural Biosecurity Center (NABC) at Kansas State University. We would like to give special thanks to the anonymous editor and reviewer for their comments. We are grateful to Jason Coleman, Regina M. Beard, Livia Olsen, and Kelebogile Olifant for their help on bibliography research. We would like to give thanks to Duygu Balcan, Phillip Schumm, Faryad Darabi Sahneh, Anton Lyubinin, and Getahun Agga for the help in producing the paper, and Kristine Bennett for answering questions on entomology.

Appendix

Exact Computation of R_0

We compute R_0 as the spectral radius of the next generation matrix of the entire system [14, 29], $R_0 = \rho(FV^{-1})$. Before applying the method we need to verify that the five assumptions in [16] are satisfied [23]. First, the equations in the system are reordered so that the first m ($m = 9$) compartments correspond to infected individuals.

$$\frac{dQ_1}{dt} = b_1 q_1 I_1 - \theta_1 Q_1 \quad (57)$$

$$\frac{dE_1}{dt} = \beta_{21} S_1 I_2 / N_2 - \varepsilon_1 E_1 - d_1 E_1 N_1 / K_1 \quad (58)$$

$$\frac{dI_1}{dt} = \theta_1 Q_1 + \varepsilon_1 E_1 - d_1 I_1 N_1 / K_1 \quad (59)$$

$$\frac{dE_2}{dt} = \beta_{12} S_2 I_1 / N_1 + \beta_{32} S_2 I_3 / N_3 - \varepsilon_2 E_2 - d_2 E_2 N_2 / K_2 \quad (60)$$

$$\frac{dI_2}{dt} = \varepsilon_2 E_2 - \gamma_2 I_2 - \mu_2 I_2 - d_2 I_2 N_2 / K_2 \quad (61)$$

$$\frac{dE_3}{dt} = \beta_{23} S_3 I_2 / N_2 - \varepsilon_3 E_3 - d_3 E_3 N_3 / K_3 \quad (62)$$

$$\frac{dI_3}{dt} = \varepsilon_3 E_3 - d_3 I_3 N_3 / K_3 \quad (63)$$

$$\frac{dE_4}{dt} = \beta_{14} S_4 I_1 / N_1 + f \beta_{24} S_4 I_2 / N_2 + \beta_{34} S_4 I_3 / N_3 - d_4 E_4 N_4 / K_4 - \varepsilon_4 E_4 \quad (64)$$

$$\frac{dI_4}{dt} = \varepsilon_4 E_4 - \gamma_4 I_4 - \mu_4 I_4 - d_4 I_4 N_4 / K_4 \quad (65)$$

$$\frac{dP_1}{dt} = b_1 (N_1 - q_1 I_1) - \theta_1 P_1 \quad (66)$$

$$\frac{dP_3}{dt} = b_3 N_3 - \theta_3 P_3 \quad (67)$$

$$\frac{dS_1}{dt} = \theta_1 P_1 - \beta_{21} S_1 I_2 / N_2 - d_1 S_1 N_1 / K_1 \quad (68)$$

$$\frac{dS_2}{dt} = b_2 N_2 - d_2 S_2 N_2 / K_2 - \beta_{12} S_2 I_1 / N_1 - \beta_{32} S_2 I_3 / N_3 \quad (69)$$

$$\frac{dS_3}{dt} = \theta_3 P_3 - \beta_{23} S_3 I_2 / N_2 - d_3 S_3 N_3 / K_3 \quad (70)$$

$$\frac{dS_4}{dt} = b_4 N_4 - \beta_{14} S_4 I_1 / N_1 - f \beta_{24} S_4 I_2 / N_2 - \beta_{34} S_4 I_3 / N_3 - d_4 S_4 N_4 / K_4 \quad (71)$$

$$\frac{dR_2}{dt} = \gamma_2 I_2 - d_2 R_2 N_2 / K_2 \quad (72)$$

$$\frac{dR_4}{dt} = \gamma_4 I_4 - d_4 R_4 N_4 / K_4 \quad (73)$$

The above system can be written as $f_k(x) = \mathcal{F}_k(x) - \mathcal{V}_k(x)$, $k = 17$

where

$$x = [Q_1 \ E_1 \ I_1 \ E_2 \ I_2 \ E_3 \ I_3 \ E_4 \ I_4 \ P_1 \ P_3 \ S_1 \ S_2 \ S_3 \ S_4 \ R_2 \ R_4]^T,$$

is the number of individuals in each compartment.

and

$$X_S = \begin{bmatrix} Q_1^0 & E_1^0 & I_1^0 & E_2^0 & I_2^0 & E_3^0 & I_3^0 & E_4^0 & I_4^0 & P_1^0 & P_3^0 & S_1^0 & S_2^0 & S_3^0 & S_4^0 & R_2^0 & R_4^0 \end{bmatrix}^T \\ = \begin{bmatrix} 0 & 0 & 0 & 0 & 0 & 0 & 0 & 0 & 0 & \frac{b_1^0 K_1}{d_1 \theta_1} & \frac{b_3^0 K_3}{d_3 \theta_3} & \frac{b_1 K_1}{d_1} & \frac{b_2 K_2}{d_2} & \frac{b_3 K_3}{d_3} & \frac{b_4 K_4}{d_4} & 0 & 0 \end{bmatrix}^T,$$

is the set of disease free states.

$\mathcal{F}(x)$, $\mathcal{V}^-(x)$, and $\mathcal{V}^+(x)$ are given in the following.

$$\begin{array}{lll} \mathcal{F}_1 = b_1 q_1 I_1, & \mathcal{V}_1^- = \theta_1 Q_1 & \\ \mathcal{F}_2 = \beta_{21} S_1 I_2 / N_2, & \mathcal{V}_2^- = \varepsilon_1 E_1 + d_1 E_1 N_1 / K_1 & \\ \mathcal{F}_3 = 0, & \mathcal{V}_3^- = d_1 I_1 N_1 / K_1, & \mathcal{V}_3^+ = \theta_1 Q_1 + \varepsilon_1 E_1 \\ \mathcal{F}_4 = \beta_{12} S_2 I_1 / N_1 + \beta_{32} S_2 I_3 / N_3, & \mathcal{V}_4^- = \varepsilon_2 E_2 + d_2 E_2 N_2 / K_2 & \\ \mathcal{F}_5 = 0, & \mathcal{V}_5^- = \gamma_2 I_2 + \mu_2 I_2 + d_2 I_2 N_2 / K_2, & \mathcal{V}_5^+ = \varepsilon_2 E_2 \\ \mathcal{F}_6 = \beta_{23} S_3 I_2 / N_2, & \mathcal{V}_6^- = \varepsilon_3 E_3 + d_3 E_3 N_3 / K_3 & \\ \mathcal{F}_7 = 0, & \mathcal{V}_7^- = d_3 I_3 N_3 / K_3 & \mathcal{V}_7^+ = \varepsilon_3 E_3, \\ \mathcal{F}_8 = \beta_{14} S_4 I_1 / N_1 + f \beta_{24} S_4 I_2 / N_2, & \mathcal{V}_8^- = d_4 E_4 N_4 / K_4 + \varepsilon_4 E_4 & \\ & + \beta_{34} S_4 I_3 / N_3, & \\ \mathcal{F}_9 = 0, & \mathcal{V}_9^- = \gamma_4 I_4 + \mu_4 I_4 + d_4 I_4 N_4 / K_4, & \mathcal{V}_9^+ = \varepsilon_4 E_4 \\ \mathcal{F}_{10} = 0, & \mathcal{V}_{10}^- = b_1 q_1 I_1 + \theta_1 P_1, & \mathcal{V}_{10}^+ = b_1 N_1 \\ \mathcal{F}_{11} = 0, & \mathcal{V}_{11}^- = \theta_3 P_3, & \mathcal{V}_{11}^+ = b_3 N_3 \\ \mathcal{F}_{12} = 0, & \mathcal{V}_{12}^- = \beta_{21} S_1 I_2 / N_2 + d_1 S_1 N_1 / K_1, & \mathcal{V}_{12}^+ = \theta_1 P_1 \\ \mathcal{F}_{13} = 0, & \mathcal{V}_{13}^- = d_2 S_2 N_2 / K_2 + \beta_{12} S_2 I_1 / N_1 + \beta_{32} S_2 I_3 / N_3, & \mathcal{V}_{13}^+ = b_2 N_2 \\ \mathcal{F}_{14} = 0, & \mathcal{V}_{14}^- = \beta_{23} S_3 I_2 / N_2 + d_3 S_3 N_3 / K_3, & \mathcal{V}_{14}^+ = \theta_3 P_3 \\ \mathcal{F}_{15} = 0, & \mathcal{V}_{15}^- = \beta_{14} S_4 I_1 / N_1 + f \beta_{24} S_4 I_2 / N_2, & \mathcal{V}_{15}^+ = b_4 N_4 \\ & + \beta_{34} S_4 I_3 / N_3 + d_4 S_4 N_4 / K_4 & \\ \mathcal{F}_{16} = 0, & \mathcal{V}_{16}^- = d_2 R_2 N_2 / K_2 & \mathcal{V}_{16}^+ = \gamma_2 I_2 \\ \mathcal{F}_{17} = 0, & \mathcal{V}_{17}^- = d_4 R_4 N_4 / K_4, & \mathcal{V}_{17}^+ = \gamma_4 I_4 \end{array}$$

As it can be easily seen, the following five assumptions [16] are satisfied.

- (A1) if $x \geq 0$, then $\mathcal{F}_i, \mathcal{V}_i^+, \mathcal{V}_i^- \geq 0$ for $i = 1, \dots, 17$.
- (A2) if $x_i = 0$, then $\mathcal{V}_i^- = 0$; in particular, if $x \in X_S$, then $\mathcal{V}_i^- = 0$ for $i = 1, \dots, 9$.
- (A3) $\mathcal{F}_i = 0$ if $i > 9$; there are no new infections in uninfected compartments.

(A4) if $x \in X_s$, then $\mathcal{F}_i(x) = 0$ and $\mathcal{V}_i^+(x) = 0$ for $i = 1, \dots, 9$.

(A5) if $\mathcal{F}(x)$ is set to 0, then all eigenvalues of $Df(x_0)$ have negative real parts.

To construct the next generation matrix, we only consider infected and exposed compartments. The equations are transformed as follows.

$$\frac{d}{dt} \begin{bmatrix} Q_1 \\ E_1 \\ I_1 \\ E_2 \\ I_2 \\ E_3 \\ I_3 \\ E_4 \\ I_4 \end{bmatrix} = \mathcal{F} - \mathcal{V} = \begin{bmatrix} b_1 q_1 I_1 \\ \beta_{21} S_1 I_2 / N_2 \\ 0 \\ \beta_{12} S_2 I_1 / N_1 + \beta_{32} S_2 I_3 / N_3 \\ 0 \\ \beta_{23} S_3 I_2 / N_2 \\ 0 \\ \beta_{14} S_4 I_1 / N_1 + f \beta_{24} S_4 I_2 / N_2 + \beta_{34} S_4 I_3 / N_3 \\ 0 \end{bmatrix} - \begin{bmatrix} \theta_1 Q_1 \\ d_1 E_1 N_1 / K_1 + \varepsilon_1 E_1 \\ -\theta_1 Q_1 + d_1 I_1 N_1 / K_1 - \varepsilon_1 E_1 \\ d_2 E_2 N_2 / K_2 + \varepsilon_2 E_2 \\ -\varepsilon_2 E_2 + d_2 I_2 N_2 / K_2 + \gamma_2 I_2 + \mu_2 I_2 \\ d_3 E_3 N_3 / K_3 + \varepsilon_3 E_3 \\ d_3 I_3 N_3 / K_3 - \varepsilon_3 E_3 \\ d_4 E_4 N_4 / K_4 + \varepsilon_4 E_4 \\ d_4 I_4 N_4 / K_4 - \varepsilon_4 E_4 + \gamma_4 I_4 + \mu_4 I_4 \end{bmatrix},$$

The equation system is nonlinear; we linearize it, deriving the two Jacobian matrices. First, the partial derivative of \mathcal{F} with respect to each variable at the disease free equilibrium is as follows [16].

$$F = \begin{bmatrix} 0 & 0 & b_1 q_1 & 0 & 0 & 0 & 0 & 0 & 0 & 0 \\ 0 & 0 & 0 & 0 & \beta_{21} \frac{S_1^0}{N_2^0} & 0 & 0 & 0 & 0 & 0 \\ 0 & 0 & 0 & 0 & 0 & 0 & 0 & 0 & 0 & 0 \\ 0 & 0 & \beta_{12} \frac{S_2^0}{N_1^0} & 0 & 0 & 0 & \beta_{32} \frac{S_2^0}{N_3^0} & 0 & 0 & 0 \\ 0 & 0 & 0 & 0 & 0 & 0 & 0 & 0 & 0 & 0 \\ 0 & 0 & 0 & 0 & \beta_{23} \frac{S_3^0}{N_2^0} & 0 & 0 & 0 & 0 & 0 \\ 0 & 0 & 0 & 0 & 0 & 0 & 0 & 0 & 0 & 0 \\ 0 & 0 & \beta_{14} \frac{S_4^0}{N_1^0} & 0 & f \beta_{24} \frac{S_4^0}{N_2^0} & 0 & \beta_{34} \frac{S_4^0}{N_3^0} & 0 & 0 & 0 \\ 0 & 0 & 0 & 0 & 0 & 0 & 0 & 0 & 0 & 0 \end{bmatrix} \quad (74)$$

Second, the partial derivative of \mathcal{V} with respect to each variable at disease free equilibrium is as follows.

$$V = \begin{bmatrix} \theta_1 & 0 & 0 & 0 & 0 & 0 & 0 & 0 & 0 & 0 \\ 0 & b_1 + \varepsilon_1 & 0 & 0 & 0 & 0 & 0 & 0 & 0 & 0 \\ -\theta_1 & -\varepsilon_1 & b_1 & 0 & 0 & 0 & 0 & 0 & 0 & 0 \\ 0 & 0 & 0 & b_2 + \varepsilon_2 & 0 & 0 & 0 & 0 & 0 & 0 \\ 0 & 0 & 0 & -\varepsilon_2 & b_2 + \gamma_2 + \mu_2 & 0 & 0 & 0 & 0 & 0 \\ 0 & 0 & 0 & 0 & 0 & b_3 + \varepsilon_3 & 0 & 0 & 0 & 0 \\ 0 & 0 & 0 & 0 & 0 & -\varepsilon_3 & b_3 & 0 & 0 & 0 \\ 0 & 0 & 0 & 0 & 0 & 0 & 0 & b_4 + \varepsilon_4 & 0 & 0 \\ 0 & 0 & 0 & 0 & 0 & 0 & 0 & -\varepsilon_4 & b_4 + \gamma_4 + \mu_4 & 0 \end{bmatrix} \quad (75)$$

The inverse of matrix V is computed as follows.

$$V^{-1} = \begin{bmatrix} \frac{1}{\theta_1} & 0 & 0 & 0 & 0 & 0 & 0 & 0 & 0 & 0 \\ 0 & \frac{1}{b_1 + \varepsilon_1} & 0 & 0 & 0 & 0 & 0 & 0 & 0 & 0 \\ \frac{1}{b_1} & \frac{\varepsilon_1}{b_1(b_1 + \varepsilon_1)} & \frac{1}{b_1} & 0 & 0 & 0 & 0 & 0 & 0 & 0 \\ 0 & 0 & 0 & \frac{1}{b_2 + \varepsilon_2} & 0 & 0 & 0 & 0 & 0 & 0 \\ 0 & 0 & 0 & \frac{\varepsilon_2}{(b_2 + \varepsilon_2)(b_2 + \gamma_2 + \mu_2)} & \frac{1}{b_2 + \gamma_2 + \mu_2} & 0 & 0 & 0 & 0 & 0 \\ 0 & 0 & 0 & 0 & 0 & \frac{1}{b_3 + \varepsilon_3} & 0 & 0 & 0 & 0 \\ 0 & 0 & 0 & 0 & 0 & \frac{\varepsilon_3}{b_3(b_3 + \varepsilon_3)} & \frac{1}{b_3} & 0 & 0 & 0 \\ 0 & 0 & 0 & 0 & 0 & 0 & 0 & \frac{1}{b_4 + \varepsilon_4} & 0 & 0 \\ 0 & 0 & 0 & 0 & 0 & 0 & 0 & \frac{\varepsilon_4}{(b_4 + \varepsilon_4)(b_4 + \gamma_4 + \mu_4)} & \frac{1}{b_4 + \gamma_4 + \mu_4} & 0 \end{bmatrix}$$

Finally, the next generation matrix, which is the product FV^{-1} , is as follows.

$$FV^{-1} = \begin{bmatrix} A_1 & B_1 & A_1 & 0 & 0 & 0 & 0 & 0 & 0 \\ 0 & 0 & 0 & C_1 & D_1 & 0 & 0 & 0 & 0 \\ 0 & 0 & 0 & 0 & 0 & 0 & 0 & 0 & 0 \\ E_1 & F_1 & G_1 & 0 & 0 & H_1 & I_1 & 0 & 0 \\ 0 & 0 & 0 & 0 & 0 & 0 & 0 & 0 & 0 \\ 0 & 0 & 0 & J_1 & L_1 & 0 & 0 & 0 & 0 \\ 0 & 0 & 0 & 0 & 0 & 0 & 0 & 0 & 0 \\ M_1 & N_1 & P_1 & Q_1 & R_1 & S_1 & T_1 & 0 & 0 \\ 0 & 0 & 0 & 0 & 0 & 0 & 0 & 0 & 0 \end{bmatrix}$$

where:

$$\begin{aligned} A_1 &= q_1 \\ B_1 &= \frac{q_1 \varepsilon_1}{b_1 + \varepsilon_1} \\ C_1 &= \frac{\varepsilon_2 \beta_{21} b_1 K_1 d_2}{(b_2 + \varepsilon_2)(b_2 + \gamma_2 + \mu_2) d_1 b_2 K_2} \\ D_1 &= \frac{\beta_{21} b_1 K_1 d_2}{(b_2 + \gamma_2 + \mu_2) d_1 b_2 K_2} \\ E_1 &= \frac{\beta_{12} b_2 K_2 d_1}{b_1^2 d_2 K_1} \\ F_1 &= \frac{\varepsilon_1 \beta_{12} b_2 K_2 d_1}{(b_1 + \varepsilon_1) b_1^2 d_2 K_1} \\ G_1 &= \frac{\beta_{12} b_2 K_2 d_1}{b_1^2 d_2 K_1} \\ H_1 &= \frac{\varepsilon_3 \beta_{32} b_2 K_2 d_3}{(b_3 + \varepsilon_3) b_3^2 d_2 K_3} \\ I_1 &= \frac{\beta_{32} b_2 K_2 d_3}{b_3^2 d_2 K_3} \\ J_1 &= \frac{\varepsilon_2 b_3 K_3 d_2 \beta_{23}}{(b_2 + \varepsilon_2)(b_2 + \gamma_2 + \mu_2) d_3 b_2 K_2} \\ L_1 &= \frac{b_3 K_3 d_2 \beta_{23}}{(b_2 + \gamma_2 + \mu_2) d_3 b_2 K_2} \\ M_1 &= \frac{b_4 K_4 d_1 \beta_{14}}{b_1^2 d_4 K_1} \\ N_1 &= \frac{\varepsilon_1 \beta_{14} b_4 K_4 d_1}{(b_1 + \varepsilon_1) b_1^2 d_4 K_1} \\ P_1 &= \frac{b_4 d_1 K_4 \beta_{14}}{b_1^2 d_4 K_1} \\ Q_1 &= \frac{f \varepsilon_2 b_4 K_4 d_2 \beta_{24}}{(b_2 + \varepsilon_2)(b_2 + \gamma_2 + \mu_2) d_4 b_2 K_2} \\ R_1 &= \frac{f b_4 K_4 d_2 \beta_{24}}{(b_2 + \gamma_2 + \mu_2) d_4 b_2 K_2} \\ S_1 &= \frac{\varepsilon_3 b_4 K_4 d_3 \beta_{34}}{(b_3 + \varepsilon_3) b_3^2 d_4 K_3} \\ T_1 &= \frac{b_4 K_4 d_3 \beta_{34}}{b_3^2 K_3 d_4} \end{aligned}$$

Recall that the reproduction number is the spectral radius of FV^{-1} , we compute the nine eigenvalues λ_i of FV^{-1} to select the one with maximum magnitude.

$$|FV^{-1} - \lambda I| = \begin{vmatrix} A_1 - \lambda & B_1 & A_1 & 0 & 0 & 0 & 0 & 0 & 0 \\ 0 & -\lambda & 0 & C_1 & D_1 & 0 & 0 & 0 & 0 \\ 0 & 0 & -\lambda & 0 & 0 & 0 & 0 & 0 & 0 \\ E_1 & F_1 & G_1 & -\lambda & 0 & H_1 & I_1 & 0 & 0 \\ 0 & 0 & 0 & 0 & -\lambda & 0 & 0 & 0 & 0 \\ 0 & 0 & 0 & J_1 & L_1 & -\lambda & 0 & 0 & 0 \\ 0 & 0 & 0 & 0 & 0 & 0 & -\lambda & 0 & 0 \\ M_1 & N_1 & P_1 & Q_1 & R_1 & S_1 & T_1 & -\lambda & 0 \\ 0 & 0 & 0 & 0 & 0 & 0 & 0 & 0 & -\lambda \end{vmatrix}$$

$$= -\lambda^6[\lambda^3 - A_1\lambda^2 - (C_1F_1 + J_1H_1)\lambda + (H_1A_1J_1 + A_1C_1F_1 - B_1C_1E_1)] \quad (76)$$

$$B_1C_1E_1 = \frac{q_1\varepsilon_1\varepsilon_2\beta_{12}\beta_{21}}{b_1(b_1 + \varepsilon_1)(b_2 + \varepsilon_2)(b_2 + \mu_2 + \gamma_2)} \quad (77)$$

$$A_1C_1F_1 = \frac{q_1\varepsilon_1\varepsilon_2\beta_{12}\beta_{21}}{b_1(b_1 + \varepsilon_1)(b_2 + \varepsilon_2)(b_2 + \mu_2 + \gamma_2)} \quad (78)$$

Because $B_1C_1E_1 = A_1C_1F_1$ as shown in Equation (78) and (77), equation (76) can be rewritten as follows.

$$-\lambda^6[\lambda^3 - A_1\lambda^2 - (C_1F_1 + J_1H_1)\lambda + H_1A_1J_1] = 0 \quad (79)$$

Equation (79) has six zero roots. We only need to solve the following equation to find $\max |\lambda_i|$ ($i = 1, 2, 3$).

$$\lambda^3 - A_1\lambda^2 - (C_1F_1 + J_1H_1)\lambda + H_1A_1J_1 = 0 \quad (80)$$

Equivalently,

$$\lambda^3 - q_1\lambda^2 - \left[\frac{\varepsilon_1\varepsilon_2\beta_{21}\beta_{12}}{b_1(b_1 + \varepsilon_1)(b_2 + \varepsilon_2)(b_2 + \mu_2 + \gamma_2)} + \frac{\varepsilon_2\varepsilon_3\beta_{23}\beta_{32}}{b_3(b_3 + \varepsilon_3)(b_2 + \varepsilon_2)(b_2 + \mu_2 + \gamma_2)} \right] \lambda + \frac{q_1\varepsilon_2\varepsilon_3\beta_{23}\beta_{32}}{b_3(b_3 + \varepsilon_3)(b_2 + \varepsilon_2)(b_2 + \mu_2 + \gamma_2)} = 0 \quad (81)$$

We calculate the reproduction number numerically with 5000 different sets of parameters uniformly distributed within the range in [18]. The histogram of the reproduction number is shown in Figure 7. From the histogram, we can see that R_0 can be greater or smaller than 1. In particular, the mean is 1.17 and the maximum is 3.68, respectively.

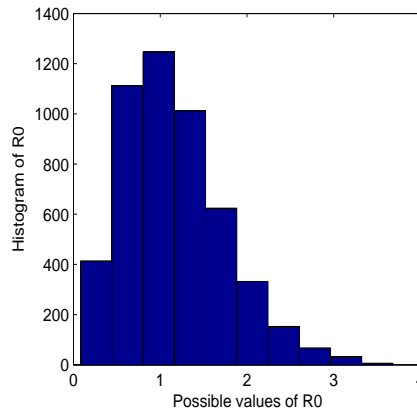


Figure 7: Histogram of the reproduction number, the mean is 1.17, the maximum is 3.68

Upper and Lower Bound for R_0

Although we are able to only obtain the exact expression of R_0 numerically, we determine the lower bound and the upper bound of R_0 in the following.

$$|FV^{-1} - \lambda I| = \begin{vmatrix} A_1 - \lambda & B_1 & A_1 & 0 & 0 & 0 & 0 & 0 & 0 \\ 0 & -\lambda & 0 & C_1 & D_1 & 0 & 0 & 0 & 0 \\ 0 & 0 & -\lambda & 0 & 0 & 0 & 0 & 0 & 0 \\ E_1 & F_1 & G_1 & -\lambda & 0 & H_1 & I_1 & 0 & 0 \\ 0 & 0 & 0 & 0 & -\lambda & 0 & 0 & 0 & 0 \\ 0 & 0 & 0 & J_1 & L_1 & -\lambda & 0 & 0 & 0 \\ 0 & 0 & 0 & 0 & 0 & 0 & -\lambda & 0 & 0 \\ M_1 & N_1 & P_1 & Q_1 & R_1 & S_1 & T_1 & -\lambda & 0 \\ 0 & 0 & 0 & 0 & 0 & 0 & 0 & 0 & -\lambda \end{vmatrix} = -\lambda^5 \begin{vmatrix} A_1 - \lambda & B_1 & 0 & 0 \\ 0 & -\lambda & C_1 & 0 \\ E_1 & F_1 & -\lambda & H_1 \\ 0 & 0 & J_1 & -\lambda \end{vmatrix} = -\lambda^5 |\mathcal{A} - \lambda I|$$

Where:

$$\mathcal{A} = \begin{bmatrix} A_1 & B_1 & 0 & 0 \\ 0 & 0 & C_1 & 0 \\ E_1 & F_1 & 0 & H_1 \\ 0 & 0 & J_1 & 0 \end{bmatrix} = \begin{bmatrix} q_1 & \frac{q_1 \varepsilon_1}{b_1 + \varepsilon_1} & 0 & 0 \\ 0 & 0 & \frac{\varepsilon_2 \beta_{21} b_1 K_1 d_2}{(b_2 + \varepsilon_2)(b_2 + \gamma_2 + \mu_2) d_1 b_2 K_2} & 0 \\ \frac{\beta_{12} b_2 K_2 d_1}{b_1^2 d_2 K_1} & \frac{\varepsilon_1 \beta_{12} b_2 K_2 d_1}{(b_1 + \varepsilon_1) b_1^2 d_2 K_1} & 0 & \frac{\varepsilon_3 \beta_{32} b_2 K_2 d_3}{(b_3 + \varepsilon_3) b_3^2 d_2 K_3} \\ 0 & 0 & \frac{\varepsilon_2 b_3 K_3 d_2 \beta_{23}}{(b_2 + \varepsilon_2)(b_2 + \gamma_2 + \mu_2) d_3 b_2 K_2} & 0 \end{bmatrix}$$

Matrix FV^{-1} has five zero roots. To find out the spectral radius of FV^{-1} , we only need to find out the spectral radius of matrix \mathcal{A} which can be rewritten as follows.

$$\mathcal{A} = \begin{bmatrix} 0 & 0 & 0 & 0 \\ 0 & 0 & \frac{\varepsilon_2 \beta_{21} b_1 K_1 d_2}{(b_2 + \varepsilon_2)(b_2 + \gamma_2 + \mu_2) d_1 b_2 K_2} & 0 \\ \frac{\beta_{12} b_2 K_2 d_1}{b_1^2 d_2 K_1} & \frac{\varepsilon_1 \beta_{12} b_2 K_2 d_1}{(b_1 + \varepsilon_1) b_1^2 d_2 K_1} & 0 & \frac{\varepsilon_3 \beta_{32} b_2 K_2 d_3}{(b_3 + \varepsilon_3) b_3^2 d_2 K_3} \\ 0 & 0 & \frac{\varepsilon_2 b_3 K_3 d_2 \beta_{23}}{(b_2 + \varepsilon_2)(b_2 + \gamma_2 + \mu_2) d_3 b_2 K_2} & 0 \end{bmatrix} + \begin{bmatrix} q_1 & \frac{q_1 \varepsilon_1}{b_1 + \varepsilon_1} & 0 & 0 \\ 0 & 0 & 0 & 0 \\ 0 & 0 & 0 & 0 \\ 0 & 0 & 0 & 0 \end{bmatrix} = \mathcal{B} + C$$

\mathcal{B} is the first matrix and C is the second matrix. The matrix C has three multiple eigenvalues $\lambda_2 = \lambda_3 = \lambda_4 = 0$. Since $\text{Rank}(\lambda_i I - C)|_{\lambda_2 = \lambda_3 = \lambda_4 = 0} = 1$, there are three linear independent eigenvectors corresponding to zero eigenvalue. Overall, matrix C has four linear independent eigenvectors. Therefore, matrix C can be diagonalized as follows.

$$C = P \begin{bmatrix} q_1 & 0 & 0 & 0 \\ 0 & 0 & 0 & 0 \\ 0 & 0 & 0 & 0 \\ 0 & 0 & 0 & 0 \end{bmatrix} P^{-1},$$

where:

$$P = \begin{bmatrix} 1 & -\frac{q_1 \varepsilon_1}{b_1 + \varepsilon_1} & 0 & 0 \\ 0 & q_1 & 0 & 0 \\ 0 & 0 & 1 & 0 \\ 0 & 0 & 0 & 1 \end{bmatrix}, \quad P^{-1} = \begin{bmatrix} 1 & \frac{\varepsilon_1}{b_1 + \varepsilon_1} & 0 & 0 \\ 0 & \frac{1}{q_1} & 0 & 0 \\ 0 & 0 & 1 & 0 \\ 0 & 0 & 0 & 1 \end{bmatrix},$$

Substitute C in the expression of $\mathcal{A} = \mathcal{B} + C$.

$$\mathcal{A} = P(P^{-1} \mathcal{B} P + \begin{bmatrix} q_1 & 0 & 0 & 0 \\ 0 & 0 & 0 & 0 \\ 0 & 0 & 0 & 0 \\ 0 & 0 & 0 & 0 \end{bmatrix}) P^{-1} = P(X + Y) P^{-1}$$

where

$$X = P^{-1} \mathcal{B} P = \begin{bmatrix} 0 & 0 & \frac{\varepsilon_1 \varepsilon_2 \beta_{21} b_1 K_1 d_1}{(b_1 + \varepsilon_1)(b_2 + \varepsilon_2)(b_2 + \gamma_2 + \mu_2) d_1 b_2 K_2} & 0 \\ 0 & 0 & \frac{\varepsilon_2 \beta_{21} b_1 K_1 d_2}{q_1 (b_2 + \varepsilon_2)(b_2 + \gamma_2 + \mu_2) d_1 b_2 K_2} & 0 \\ 0 & \frac{\beta_{21} b_2 K_2 d_1}{b_1^2 d_2 K_1} & 0 & \frac{\varepsilon_3 \beta_{32} b_2 K_2 d_3}{(b_3 + \varepsilon_3) d_2 b_3^2 K_3} \\ 0 & 0 & \frac{\varepsilon_2 \beta_{23} b_3 K_3 d_2}{(b_2 + \varepsilon_2)(b_2 + \gamma_2 + \mu_2) d_3 b_2 K_2} & 0 \end{bmatrix}, \quad Y = \begin{bmatrix} q_1 & 0 & 0 & 0 \\ 0 & 0 & 0 & 0 \\ 0 & 0 & 0 & 0 \\ 0 & 0 & 0 & 0 \end{bmatrix}.$$

Matrix Y is a 4×4 nonnegative diagonal matrix ($Y_{ij} = 0$ for $i \neq j$) and $0 \leq Y_{ii} < q_1 = \max_j v_{jj} < \infty$, ($i = 2, 3, 4$), and matrix X is nonnegative. Therefore, $\rho(X) \leq \rho(X + Y) \leq \rho(X) + q_1$ according to Theorem 1. in [10]. The eigenvalues of matrix $X + Y$

are the same as those of \mathcal{A} because the two matrices are similar. Similarly, the eigenvalues of matrix X are the same as those of matrix \mathcal{B} .

$$\rho(X + Y) = \rho(FV^{-1}) = R_0$$

$$\rho(X) = \sqrt{\frac{\varepsilon_2}{(b_2 + \varepsilon_2)(b_2 + \gamma_2 + \mu_2)} \left[\frac{\varepsilon_1 \beta_{12} \beta_{21}}{b_1(b_1 + \varepsilon_1)} + \frac{\varepsilon_3 \beta_{32} \beta_{23}}{b_3(b_3 + \varepsilon_3)} \right]}$$

If we only count the horizontal transmission and denote the new F (resp. V) by F_H (resp. V_H), F_H and V_H are as follows.

$$F_H = \begin{bmatrix} 0 & 0 & 0 & \beta_{21} \frac{S_1^0}{N_2^0} & 0 & 0 & 0 & 0 \\ 0 & 0 & 0 & 0 & 0 & 0 & 0 & 0 \\ 0 & \beta_{12} \frac{S_2^0}{N_1^0} & 0 & 0 & 0 & \beta_{32} \frac{S_2^0}{N_3^0} & 0 & 0 \\ 0 & 0 & 0 & 0 & 0 & 0 & 0 & 0 \\ 0 & 0 & 0 & \beta_{23} \frac{S_3^0}{N_2^0} & 0 & 0 & 0 & 0 \\ 0 & 0 & 0 & 0 & 0 & 0 & 0 & 0 \\ 0 & \beta_{14} \frac{S_4^0}{N_1^0} & 0 & \beta_{24} \frac{S_4^0}{N_2^0} & 0 & \beta_{34} \frac{S_4^0}{N_3^0} & 0 & 0 \\ 0 & 0 & 0 & 0 & 0 & 0 & 0 & 0 \end{bmatrix},$$

$$V_H = \begin{bmatrix} \frac{d_1 N_1^0}{K_1} + \varepsilon_1 & 0 & 0 & 0 & 0 & 0 & 0 & 0 \\ -\varepsilon_1 & \frac{d_1 N_1^0}{K_1} & 0 & 0 & 0 & 0 & 0 & 0 \\ 0 & 0 & \frac{d_2 N_2^0}{K_2} + \varepsilon_2 & 0 & 0 & 0 & 0 & 0 \\ 0 & 0 & -\varepsilon_2 & \frac{d_2 N_2^0}{K_2} + \gamma_2 + \mu_2 & 0 & 0 & 0 & 0 \\ 0 & 0 & 0 & 0 & \frac{d_3 N_3^0}{K_3} + \varepsilon_3 & 0 & 0 & 0 \\ 0 & 0 & 0 & 0 & -\varepsilon_3 & \frac{d_3 N_3^0}{K_3} & 0 & 0 \\ 0 & 0 & 0 & 0 & 0 & 0 & \frac{d_4 N_4^0}{K_4} + \varepsilon_4 & 0 \\ 0 & 0 & 0 & 0 & 0 & 0 & -\varepsilon_4 & \frac{d_4 N_4^0}{K_4} + \gamma_4 + \mu_4 \end{bmatrix}$$

By calculation,

$$R_0^H = \rho(F_H V_H^{-1}) = \sqrt{\frac{\varepsilon_2}{(b_2 + \varepsilon_2)(b_2 + \gamma_2 + \mu_2)} \left[\frac{\varepsilon_1 \beta_{12} \beta_{21}}{b_1(b_1 + \varepsilon_1)} + \frac{\varepsilon_3 \beta_{32} \beta_{23}}{b_3(b_3 + \varepsilon_3)} \right]} = \rho(X)$$

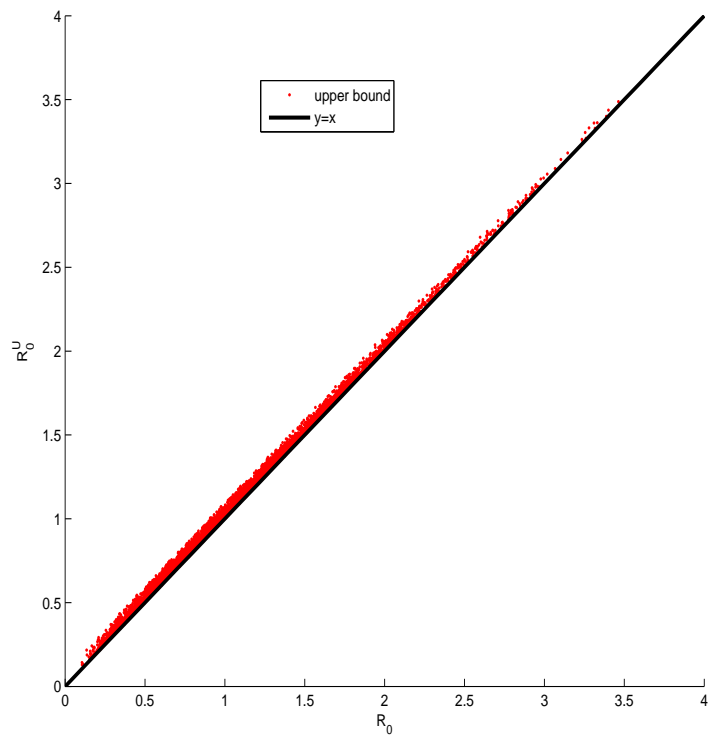
Therefore,

$$R_0^H \leq R_0 \leq R_0^H + q_1 \quad (82)$$

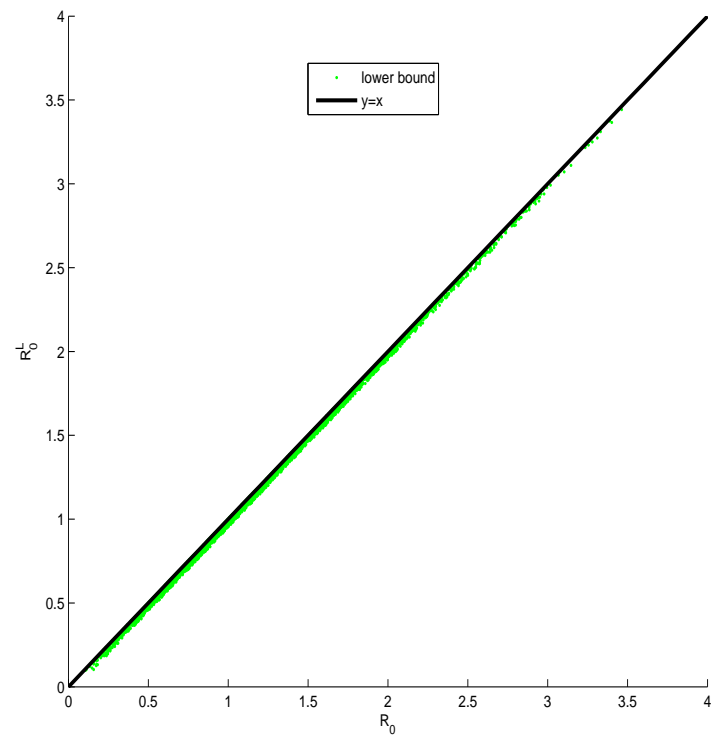
We denote R_0^H and $R_0^H + q_1$ as R_0^L and R_0^U , respectively.

Numerical Comparison among R_0 , R_0^L , and R_0^U

R_0^H and $R_0^H + q_1$ are the lower bound and the upper bound of R_0 , respectively. Therefore, $R_0^H + q_1 < 1 \Rightarrow R_0 < 1$, and $R_0^H > 1 \Rightarrow R_0 > 1$. To verify that the derived bounds are tight, we perform extensive simulations using 5000 sets of parameters uniformly distributed within the range defined in [18]. In Figure 8(a) and 8(b), $R_0^U = R_0^H + q_1$ vs. R_0 and $R_0^L = R_0^H$ vs. R_0 are plotted, respectively. First, the difference between the exact values and each bound is very small. In fact, the red and green points lay very close to the line $y = x$. Additionally, in the case of the upper bound, the red points are just slightly above the line $y = x$, while in the case of the lower bound, the green points are just slightly below the line $y = x$.



(a) The reproduction number and its upper bound.



(b) The reproduction number and its lower bound.

Figure 8: The reproduction number and its upper and lower bound

Biological Interpretation of Bounds for R_0

The bounds for R_0 , as given in inequalities (26), can be interpreted biologically as follows. The lower bound, R_0^H , is the reproduction number for horizontal transmission because $R_0^H = \rho(F_H V_H^{-1})$, where $\rho(F_H V_H^{-1})$ represents the spectral radius of the next generation matrix for horizontal transmission $F_H V_H^{-1}$. The upper bound is given by the sum of R_0^H and a second term that is only related to vertical transmission, i.e. from mothers to their offspring in the *Aedes* mosquito population.

R_0^H includes *Aedes*-livestock interaction and *Culex*-livestock interaction. More specifically, we define the reproduction number due to the interaction between *Aedes* and livestock represented by $R_0^{H(A-L)}$ as

$$R_0^{H(A-L)} = \sqrt{\frac{\varepsilon_2}{(b_2 + \varepsilon_2)(b_2 + \gamma_2 + \mu_2)} \frac{\varepsilon_1 \beta_{12} \beta_{21}}{b_1(b_1 + \varepsilon_1)}}$$

$R_0^{H(A-L)}$ can be rewritten as follows.

$$R_0^{H(A-L)} = \sqrt{\left[\frac{\beta_{12}}{d_1 \frac{N_1^*}{K_1}} \frac{\varepsilon_1}{(d_1 \frac{N_1^*}{K_1} + \varepsilon_1)} \right] \left[\frac{\beta_{21}}{(d_2 \frac{N_2^*}{K_2} + \gamma_2 + \mu_2)} \frac{\varepsilon_2}{(d_2 \frac{N_2^*}{K_2} + \varepsilon_2)} \right]} \quad (83)$$

because

$$b_1 = d_1 \frac{N_1^*}{K_1}$$

$$b_2 = d_2 \frac{N_2^*}{K_2}$$

where:

N_1^* = the total number of *Aedes* mosquitoes at disease free equilibrium.

N_2^* = the total number of livestock at disease free equilibrium.

$R_0^{H(A-L)}$ consists of the product of four terms. Each infected *Aedes* mosquito can infect $\frac{\beta_{12}}{d_1 \frac{N_1^*}{K_1}}$ susceptible livestock throughout its lifetime. Similarly, each infected livestock can infect $\frac{\beta_{21}}{d_2 \frac{N_2^*}{K_2} + \gamma_2 + \mu_2}$ susceptible *Aedes* mosquitoes during its lifetime. The probability of *Aedes* mosquitoes and livestock surviving through the incubation period to the point where they become infectious is $\frac{\varepsilon_1}{d_1 \frac{N_1^*}{K_1} + \varepsilon_1}$ and $\frac{\varepsilon_2}{d_2 \frac{N_2^*}{K_2} + \varepsilon_2}$, respectively. Therefore, $R_0^{H(A-L)}$ is the geometric mean of the average number of secondary livestock infections produced by one *Aedes* mosquito vector in the first square bracket in (83), and the average number of secondary *Aedes* mosquito vector infections produced by one livestock host in the second square bracket in (83).

Similarly, we define the reproduction number due to the interaction between *Culex* and livestock represented by $R_0^{H(C-L)}$ as

$$R_0^{H(C-L)} = \sqrt{\frac{\varepsilon_2}{(b_2 + \varepsilon_2)(b_2 + \gamma_2 + \mu_2)} \frac{\varepsilon_3 \beta_{32} \beta_{23}}{b_3(b_3 + \varepsilon_3)}}$$

We can rewrite $R_0^{H(C-L)}$ as follows.

$$R_0^{H(C-L)} = \sqrt{\left[\frac{\beta_{32}}{d_3 \frac{N_3^*}{K_3}} \frac{\varepsilon_3}{(d_3 \frac{N_3^*}{K_3} + \varepsilon_3)} \right] \left[\frac{\beta_{23}}{(d_2 \frac{N_2^*}{K_2} + \gamma_2 + \mu_2)} \frac{\varepsilon_2}{(d_2 \frac{N_2^*}{K_2} + \varepsilon_2)} \right]} \quad (84)$$

because

$$b_3 = d_3 \frac{N_3^*}{K_3}$$

where:

N_3^* = the total number of *Culex* mosquitoes at disease free equilibrium.

$R_0^{H(C-L)}$ also consists of the product of four terms. Each infected *Culex* mosquito can infect $\frac{\beta_{32}}{d_3 \frac{N_3^*}{K_3}}$ susceptible livestock throughout its lifetime. Similarly, each infected livestock can infect $\frac{\beta_{23}}{d_2 \frac{N_2^*}{K_2} + \gamma_2 + \mu_2}$ susceptible *Culex* mosquitoes. The probability of *Culex* mosquitoes surviving through the incubation period to the point where they become infectious is $\frac{\varepsilon_3}{d_3 \frac{N_3^*}{K_3} + \varepsilon_3}$. Similarly, the probability of livestock surviving through the incubation period to the point where they become infectious is $\frac{\varepsilon_2}{d_2 \frac{N_2^*}{K_2} + \varepsilon_2}$. Therefore, $R_0^{H(C-L)}$ is the geometric mean of the average number of the secondary livestock infections produced by one *Culex* mosquito vector in the first square bracket in (84), and the average number of secondary *Culex* mosquito vector infections produced by one livestock in the second square bracket in (84).

The expression (27) for R_0^H , can be rewritten as $R_0^H = \sqrt{(R_0^{H(A-L)})^2 + (R_0^{H(C-L)})^2}$, where the dependence of R_0^H on $R_0^{H(A-L)}$ and $R_0^{H(C-L)}$ is shown in Figure 9. The square root is due to the vector-host-vector viral transmission path [18? , 33]. Obviously, the horizontal reproduction number increases with the increase of each of the four terms in $R_0^{H(A-L)}$ and $R_0^{H(C-L)}$.

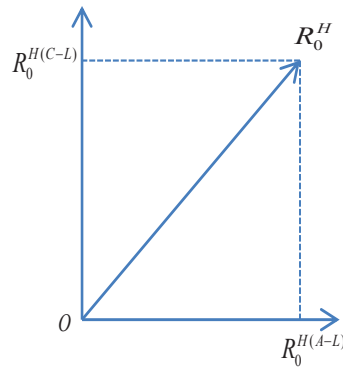


Figure 9: The interpretation of R_0^H

References

- [1] Anyamba, A., Chretien, J.P., Small, J., Tucker, C.J., Formenty, P.B., Richardson, J.H., Britch, S.C., Schnabel, D.C., Erickson, R.L., Linthicum, K.J., 2009. Prediction of a Rift Valley fever outbreak. *Proceedings of the National Academy of Sciences* 106, 955–959.
- [2] Anyamba, A., Chretien, J.P., Small, J., Tucker, C.J., Linthicum, K.J., 2006. Developing global climate anomalies suggest potential disease risks for 2006–2007. *International Journal of Health Geographics* 5, 60.
- [3] Anyamba, A., Linthicum, K.J., Mahoney, R., Tucker, C.J., 2002. Mapping potential risk of Rift Valley fever outbreaks in african savannas using vegetation index time series data. *Photogrammetric Engineering and Remote Sensing* 68, 137–145.
- [4] Anyamba, A., Linthicum, K.J., Tucker, C.J., 2001. Climate-disease connections: Rift Valley fever in kenya. *Cadernos de saude publica / Ministerio da Saude, Fundacao Oswaldo Cruz, Escola Nacional de Saude Publica* 17 Suppl, 133–140.
- [5] Balcan, D., Colizza, V., Goncalves, B., Hu, H., Ramasco, J.J., Vespignani, A., 2009. Multiscale mobility networks and the spatial spreading of infectious diseases. *Proceedings of the National Academy of Sciences of the United States of America* 106, 21484–21489.
- [6] Centers for Disease Control and Prevention (CDC), 2007. Rift Valley fever outbreak–kenya, november 2006–january 2007. *Morbidity and Mortality Weekly Report* 56, 73–76.
- [7] Chevalier, V., Lancelot, R., Thiongane, Y., Sall, B., Diaite, A., Mondet, B., 2005. Rift Valley fever in small ruminants, senegal, 2003. *Emerging Infectious Diseases* 11, 1693–1700.
- [8] Chowdhury, S.R., Scoglio, C., Hsu, W., 2010. Simulative modeling to control the foot and mouth disease epidemic. *Procedia Computer Science* 1, 2261–2270.
- [9] Clements, A.C., Pfeiffer, D.U., Martin, V., Pittiglio, C., Best, N., Thiongane, Y., 2007. Spatial risk assessment of rift Valley fever in senegal. *Vector Borne and Zoonotic Diseases (Larchmont, N.Y.)* 7, 203–216.
- [10] Cohen, J., 1979. Random evolutions and the spectral radius of a non-negative matrix. *Math. Proc. Camb. Phil. Soc.* 86, 345–350.
- [11] Davies, F.G., Martin, V., 2006. Recognizing Rift Valley fever. *Veterinaria Italiana* 42, 31–53.
- [12] Department for Environment Food and Rural Affairs, 2010. Rift Valley fever. <http://www.defra.gov.uk/foodfarm/farmanimal/diseases/atoz/riftvalleyfever/index.htm>. Accessed Nov 10, 2010.
- [13] Department of Agriculture Forestry and Fisheries of Republic of South Africa, 2010. Livestock number 96 to date. <http://www.nda.agric.za/docs/statsinfo/LivestokNo96toDate.xls>. Accessed Sep 26, 2010.
- [14] Diekmann, O., Heesterbeek, J.A.P., 2000. *Mathematical Epidemiology of Infectious Diseases: Model Building, Analysis and Interpretation* (Wiley Series in Mathematical & Computational Biology). Chapter 5, Wiley.
- [15] Disease BioPortal, . <http://fmdbioportal.ucdavis.edu>. Accessed Nov 23, 2010.
- [16] van den Driessche, P., Watmough, J., 2002. Reproduction numbers and sub-threshold endemic equilibria for compartmental models of disease transmission. *Mathematical biosciences* 180, 29–48.

- [17] Florida Department of Health, 2010. Rift Valley fever. <http://www.doh.state.fl.us/environment/medicine/arboviral/RiftValleyFever.html>. Accessed Nov 30, 2010.
- [18] Gaff, H.D., Hartley, D.M., Leahy, N.P., 2007. An epidemiological model of Rift Valley fever. *Electron. J. Diff. Eqns* 2007, 1–12.
- [19] Gong, H., Degaetano, A.T., Harrington, L.C., 2010. Climate-based models for west nile culex mosquito vectors in the northeastern us. *International Journal of Biometeorology* 55, 435–446.
- [20] Gubler, D.J., 2002. The global emergence/resurgence of arboviral diseases as public health problems. *Archives of Medical Research* 33, 330–342.
- [21] Kasari, T.R., Carr, D.A., Lynn, T.V., Weaver, J.T., 2008. Evaluation of pathways for release of Rift Valley fever virus into domestic ruminant livestock, ruminant wildlife, and human populations in the continental united states. *Journal of the American Veterinary Medical Association* 232, 514–529.
- [22] Keeling, J., Rohani, P., 2008. *Modeling infectious disease in humans and animals*. Princeton University Press.
- [23] Kim, B.N., Gordillo, L.F., Kim, Y., 2010. A model for the transmission dynamics of orientia tsutsugamushi among its natural reservoirs. *Journal of theoretical biology* 266, 154–161.
- [24] Konrad, S.K., s. N. Miller, Reeves, W.K., 2010. A spatially explicit degree-day model of Rift Valley fever transmission risk in the continental united states. *GeoJournal* .
- [25] Linacre, E.T., 1977. A simple formula for estimating evaporation rates in various climates using temperature data alone. *Agricultural Meteorology* 18, 409–424.
- [26] Linthicum, K.J., Anyamba, A., Britch, S.C., Chretien, J.P., Erickson, R.L., Small, J., Tucker, C.J., Bennett, K.E., Mayer, R.T., Schmidtman, E.T., Andreadis, T.G., Anderson, J.F., Wilson, W.C., Freier, J.E., James, A.M., Miller, R.S., Drolet, B.S., Miller, S.N., Tedrow, C.A., Bailey, C.L., Strickman, D.A., Barnard, D.R., Clark, G.G., Zou, L., 2007. A Rift Valley fever risk surveillance system for Africa using remotely sensed data: potential for use on other continents. *Veterinaria Italiana* 43, 663–674.
- [27] Linthicum, K.J., Davies, F.G., Kairo, A., Bailey, C.L., 1985. Rift Valley fever virus (family bunyaviridae, genus phlebovirus). isolations from diptera collected during an inter-epizootic period in kenya. *The Journal of Hygiene* 95, 197–209.
- [28] Martin, V., Chevalier, V., Ceccato, P., Anyamba, A., Simone, L.D., Lubroth, J., de La Rocque, S., Domenech, J., 2008. The impact of climate change on the epidemiology and control of Rift Valley fever. *Revue Scientifique et Technique (International Office of Epizootics)* 27, 413–426.
- [29] Mpeshe, S.C., Haario, H., Tchuente, J.M., 2011. A mathematical model of rift valley fever with human host. *Acta Biotheoretica* 59, 231–250.
- [30] National Climatic Data center, 2010. NOAA Satellite and Information Service. <http://www7.ncdc.noaa.gov/CDO/country>. Accessed Nov 22, 2010.
- [31] National Institute for Communicable Diseases, 2010. Interim report on the Rift Valley fever (RVF) outbreak in south africa. http://www.nicd.ac.za/?page=rift_valley_fever_outbreak&id=94. Accessed Nov 23, 2010.
- [32] Newton, E., Reiter, P., 1992. A model of the transmission of dengue fever with an evaluation of the impact of ultra-low volume (ulv) insecticide applications on dengue epidemics. *The American Journal of Tropical Medicine and Hygiene* 47, 709–720.
- [33] O. Diekmann, H.H., Metz, H., 1995. The legacy of Kermack and McKendrick. In D. Mollison, editor, *Epidemic Models: Their Structure and Relation to Data*. pages 95–115. Cambridge University Press, Cambridge, UK.
- [34] Olivier.C.G., 2004. An Analysis of the South African Beef Supply Chain: from farm to folk. Master's thesis. University of Johannesburg. South Africa.
- [35] Sellers, R.F., Pedgley, D.E., Tucker, M.R., 1982. Rift Valley fever, egypt 1977: disease spread by windborne insect vectors? *The Veterinary record* 110, 73–77.
- [36] South Africa Department of Health, 2010. Press releases 2010. <http://www.doh.gov.za/docs/pr/>. Accessed Nov 30, 2010.
- [37] Statistics South Africa, 2010a. Agricultural Census (Census of Commercial Agriculture), 2007. <http://www.statssa.gov.za/publications/statsdownload.asp?PPN=P1102&SCH=4534>. Accessed Nov 22, 2010.
- [38] Statistics South Africa, 2010b. Domestic tourism survey 2009. <http://www.statsonline.gov.za/publications/statsdownload.asp?PPN=P0352.1&SCH=4702>. Accessed Nov 23, 2010.
- [39] Statistics South Africa, 2010c. Mid-year population estimates. <http://www.statsonline.gov.za/publications/P0302/P03022010.pdf>. Accessed Nov 21, 2010.
- [40] Swanson, J.C., Morrow-Tesch, J., 2001. Cattle transport: Historical, research, and future perspectives. *Journal of Animal Science* 79, E102–E109.
- [41] Weather Underground, 2010. <http://www.wunderground.com/>. Accessed Nov 20, 2010.
- [42] Woods, C.W., Karpati, A.M., Grein, T., McCarthy, N., Gaturuku, P., Muchiri, E., Dunster, L., Henderson, A., Khan, A.S., Swanepoel, R., Bonmarin, I., Martin, L., Mann, P., Smoak, B.L., Ryan, M., Ksiazek, T.G., Arthur, R.R., Ndikuyeze, A., Agata, N.N., Peters, C.J., Force, W.H.O.H.F.T., 2002. An outbreak of Rift Valley fever in northeastern kenya, 1997–98. *Emerging Infectious Diseases* 8, 138–144.
- [43] World Animal Health Information Database, 2010. Summary of immediate notifications and follow-ups - 2010. http://www.oie.int/wahis/public.php?page=disease_immediate_summary. Accessed Oct 14, 2010.
- [44] World Health Organization, 2010. Rift Valley fever. <http://www.who.int/mediacentre/factsheets/fs207/en/>. Accessed Nov 22, 2010.
- [45] Zeller, H.G., Fontenille, D., Traore-Lamizana, M., Thiongane, Y., Digoutte, J.P., 1997. Enzootic activity of Rift Valley fever virus in senegal. *The American Journal of Tropical Medicine and Hygiene* 56, 265–272.